Journal of Research of the National Bureau of Standards Vol. 61. No. 3, September 1958 Research Paper 2894

Vibration-Rotation Bands of Ammonia:[1] 1. The Combination Bands $\nu_2+(\nu_1, \nu_3)$

William S. Benedict,[2] Earle K. Plyler, and Eugene D. Tidwell

A general discussion is given of methods used in the analysis of NH_3 vibration-rotation spectra, including the derivation of molecular constants and the determination of line strengths and line widths. Results are given for the region 2.15 to 2.48 μ (4,060 to 4,700 cm^{-1}), in which more than 800 lines have been measured. These have been analyzed into the inversion-doubled perpendicular combination band $\nu_2+\nu_3$ (ν_0=4416.908 and 4434.610 cm^{-1}; band strength=19.7 cm^{-2} atm^{-1}) and the inversion-doubled parallel combination band $\nu_1+\nu_2$ (ν_0=4293.716 and 4320.060 cm^{-1}; band strength=2.9 cm^{-2} atm^{-1}). Complete energy levels for these bands have been found up to $J=12$ and 10, respectively, permitting determinations of molecular constants, which include numerous higher-order effects involving the interaction of rotation, vibration, and inversion. The line widths range from a maximum of 0.57 cm^{-1} atm^{-1}, when $K=J$ to a minimum of <0.2 cm^{-1} atm^{-1}, when $K \ll J$.

1. Introduction

The vibration-rotation spectrum of ammonia, NH_3, has been extensively studied in the past [1],[3] and the main features of the molecular structure are understood.

It is a pyramidal molecule (symmetry C_{3v}) with the N atom approximately 0.38×10^{-8} cm above the plane of the three hydrogens, and the N-H distance approximately 1.02×10^{-8} cm. The rotational structure is that of a symmetric top. Because the pyramid is relatively flat, and the potential barrier to inversion of the nitrogen relatively low, each state is not only characterized by the six vibrational quantum numbers $v_1v_2v_3^{l_3}v_4^{l_4}$ and the rotational quantum numbers J, $K(-J\leq K\leq J)$, but also by the symmetry (s,a) with respect to the inversion plane. The inversion splitting in the ground vibrational state is $\sim$0.79 cm^{-1}.

Although the basic structural features just mentioned are established, there are a number of respects in which additional study with the high resolution afforded by modern infrared spectrometers appears desirable. Only one parallel band, the ν_2 fundamental near 10 μ has been [2] observed with resolution sufficient to separate the K-substructure of the lines, and only a partial analysis has been given [3] of the perpendicular fundamental ν_3 near 2.9 μ. For the other fundamentals, the parallel ν_1 near 3 μ, and the perpendicular ν_4 near 6 μ, only approximate values of the molecular constants are known, and there are no satisfactory analyses of any of the numerous combination and overtone bands, which have been observed extending into the visible region [4,5]. Hence neither a full set of anharmonic vibrational constants, which are needed to establish the equilibrium vibrational frequencies, nor the rotation-vibration interaction constants, which are needed to establish the equilibrium moments of inertia, are at hand. The magnitude of the inversion doubling is accurately known as a function of J and K for the ground vibrational state, as a result of measurements in the microwave region [6], but except for partial results in ν_2 [2], for which the splitting is greatly increased, and for ν_3 [3] (which appear, however, to have been incorrectly interpreted), similar data are not known for the excited vibrational states. The observation of a sufficient number of vibration-rotation bands to establish the variation of the inversion splitting with vibration-rotation would thus be desirable.

In symmetric top molecules the perpendicular bands occupy a special role, and a number of such bands must be studied in order to obtain the constants C, D^K, and ζ corresponding to rotation about the symmetry axis. This is because perpendicular bands, i. e., those in which the dipole moment changes perpendicular to the symmetry axis, occur when one of the vibrational states is doubly degenerate; and in such states there is a component of angular momentum $C_v\zeta_v$ due to vibration that interacts with the rotational angular momentum to remove the K-degeneracy. Hence the observed spacings of the lines yield $C_v(1-\zeta_v)$ rather than C_v. If ζ_v can be observed for both fundamentals, the theoretical relation $\zeta_3+\zeta_4=(B/2C)-1$ permits the calculation of C. This relation, however, is strictly true only for infinitesimal vibrations, and in order to obtain accurate molecular constants it is necessary to establish empirically the variation of the ζ with the other vibrational quantum numbers. For this purpose, as many perpendicular bands as possible must be analyzed.

In the overtone and combination bands, both perpendicular and parallel, numerous cases of near-resonance interaction are possible between the various levels of the same total symmetry. This introduces additional complications. The cases of resonance must be recognized and evaluated in order to derive the molecular potential function from the observed molecular constants. Inasmuch as it appears that it will be difficult to achieve a satisfactory derivation of the harmonic and anharmonic potential function

[1] This research was supported in part by the United States Air Force under Contract AF 18(600)-1557 monitored by the Air Force Office of Scientific Research of the Air Research and Development Command, and in part by the Atomic Energy Commission.

[2] Laboratory of Astrophysics and Physical Meteorology, The Johns Hopkins University, Baltimore, Md.

[3] Figures in brackets indicate the literature references at the end of this paper.

of the ammonia molecule from the bands of NH_3 alone, it is desirable to study the additional bands obtained with the deuterium substituted compounds ND_3, which preserves the molecular symmetry, and ND_2H and NHD_2, which are asymmetric tops. Only by such a program can one hope to obtain definitive values of the equilibrium molecular structure and potential constants.

Another respect in which the infrared spectrum of the ammonias deserves further study concerns the strength, width, shape, and possible pressure-shift of the lines. The observed spectrum, for a given condition of pressure and path length, depends upon these factors, and from a quantitative study of the variation of absorption with length and pressure it is possible to deduce the strengths, widths, and shapes of individual lines [7]. NH_3 is a particularly interesting molecule for such studies, because experiments in the microwave region have shown that the collision diameter varies markedly with the rotational quantum number. The results are in good agreement with those calculated by Anderson [8], on the basis of his general theory of collision broadening as caused by dipole-dipole forces. The same theory should apply in the infrared bands, and predicts that the widths should be nearly independent of the vibrational quantum numbers, so long as the upper state is a member of a narrow inversion doublet, as is the case for the microwave lines. When, however, the upper state has a wider inversion doubling, as in ν_2 and its combinations and overtones, the possibilities of resonant dipole interactions are reduced and the widths should be less. Because of the strong resonance interactions the half-widths are among the greatest that have been observed in molecular spectra, ranging up to 0.75 cm^{-1} at 1-atm pressure. Hence they may be measured directly in the infrared region whenever overlapping from other lines does not interfere.

The microwave collision diameters were obtained at low pressures; other interesting results were found in that region [9] at pressures from 10 cm to 1 atm. The individual lines of the inversion Q-branch are no longer resolved, but absorption in their overlapping long-wavelength wing can be measured throughout the frequency range 0.6 to 0 cm^{-1}, thus providing a test of the line shape. It is found that the absorption is considerably increased over that given by the Lorentz-Van Vleck-Weisskopf theory [10]. This has been interpreted [11] in terms of a shift of the resonance frequency of the lines toward zero frequency, as a result of the intermolecular forces. It would thus appear of great interest to study the line shape in the infrared, particularly because no gross evidence of a corresponding pressure shift of the inversion splitting toward zero is apparent [12].

An extensive series of measurements of the ammonia rotation-vibration spectrum in the region 1,700 to 7,100 cm^{-1} has been undertaken, with the purpose of clarifying as many as possible of the points mentioned above. Preliminary reports have been given of some aspects of the results [13].

In the present paper are described in detail the general methods used in analyzing the spectra, particularly those of the perpendicular-type bands, which predominate in the combination and overtone regions. These will be illustrated by the analysis of the bands in the region of 2.3 μ, where fall the combination bands $(\nu_1,\nu_3+\nu_2)$,[4] a region in which the identification of lines has been nearly complete. Some results of intensity and line-width studies in this region will also be given. Subsequent papers will deal with further problems of line width and shape, and with analysis of other bands of NH_3 and its isotopic modifications.

2. Experimental Details and Method of Analysis

The spectrometer was the 15,000-lines-per-inch grating spectrometer of the National Bureau of Standards. Its construction and operation have been described elsewhere. Wavelength calibrations were by interferometric fringes, between secondary standards of the krypton arc. Under the most favorable conditions absorption lines separated by 0.08 cm^{-1} could be resolved, and the frequency measurements are believed reliable to ± 0.03 cm^{-1} for unblended lines.

Inasmuch as it was desired to study strength, width, and shapes of the lines,[5] cells of various lengths were used; for optimum resolution a path length of 1,000 cm was required, with pressures varying from a few millimeters to 30 cm. Two shorter cells, of lengths 5.0 and 15.5 cm, with the gas at pressures from 2 cm to 1 atm, were employed to give spectra for which the lines were more nearly in the linear region of the curve of growth.

A large number of tracings of the spectrum were obtained between 2.15 and 2.5 μ (4,000 to 4,700 cm^{-1}). NH_3 lines occur throughout this region. The strongest absorption is from 4,200 to 4,500 cm^{-1}, and decreases in intensity to both directions. At the long-wavelength limit NH_3 absorption is still fairly strong at 10 m and 30-cm pressure, but is obscured by the 2.7-μ water-vapor band; near 4,700 cm^{-1} the NH_3 absorption reaches a minimum, other absorption (to be described in a subsequent paper) due to the 2.0-μ group of bands giving increasing intensity at shorter wavelengths.

The general expressions for the line positions and line strengths in NH_3 are now presented. For a review of the basic theory on which we rely, see Nielsen [14]. In his article the pyramidal XY_3 molecule, of which NH_3 is an example, is described in some detail. The present notation with a few obvious variations, will follow that recommended by Mulliken [15]. The energy levels may be written

$$T(v,p,J,K)=G(v)+F(v,J,K)\pm\frac{1}{2}E_{inv}(v,J,K), \quad (1)$$

where G is the contribution to the energy from vibration, and depends on the six vibrational quantum numbers, $V_i(i=1,2,3,4)$ and $l_i(i=3,4)$; F is the con-

[4] These bands have been observed previously [4], but with insufficient resolution to obtain accurate constants.

[5] For the methods used, see reference [7].

tribution from rotation, depending on the rotational quantum numbers J and $|K|$(and when $\Sigma l_i \neq 0$ on the sign of K), and on rotational constants, which are functions of the vibrational state; and E_{inv} is the splitting of the levels due to inversion, a function of all the quantum numbers. In eq (1) v stands for the six vibrational quantum numbers, and p for the parity of the inversion level, taking the values + and − corresponding to the sign before E_{inv}. Inasmuch as E_{inv} is written as a separate term, the vibrational energy formula refers to the average energy of the pair of inversion-doubled states, and may be written

$$G=\sum_{i=1}^{4}\nu_i v_i+\sum_{i=1}^{4}\sum_{j=1}^{4}x_{ij}(v_i-1)(v_j-1)+\sum_{i=3}^{4}\sum_{j=3}^{4}g_{ij}(v_i-l_i)(v_j-l_j)+\text{terms cubic in } v_i \pm E_{res}. \quad (2)$$

The ν_i are the observed positions of the fundamental bands ($\nu_i=1,\nu_j=0$), which for NH_3 have the approximate values (cm^{-1}) $\nu_1(A_1)=3336.9$, $\nu_2(A_1)=950.0$, $\nu_3(E)=3443.4$, $\nu_4(E)=1626.3$. The x's and g's are the anharmonic constants that it is desired to derive from measurements of combination and overtone bands ($\nu_i>1$ or $\nu_j>0$). E_{res} is an additional term that it may be necessary to introduce when two vibrational levels of like symmetry lie close together; for NH_3 the most important case of vibrational (Fermi) resonance occurs for all states with $v_1 \neq 0$, since $2\times\nu_4 \cong \nu_1$.

The rotational portion of the energy expression is

$$F(v,J,K)=B_v J(J+1)+(C_v-B_v)K^2-D_v^J J^2(J+1)^2-D_v^{JK}J(J+1)K^2-D_v^K K^4+\ \ldots \pm 2C_v\zeta_v K \mp \zeta_v^J J(J+1)K \mp \zeta_v^K K^3+\ \ldots, \quad (3)$$

where the rotational constants on the first line apply to all v, and the additional terms on the second line are needed for states where $l \neq 0$, and represent the contribution of the angular momentum of the degenerate vibrational mode, through Coriolis forces. The terms with coefficients ζ^J and ζ^K, representing the effect of centrifugal stretching on the Coriolis interaction, will be small; if higher-order interaction terms are unimportant

$$\zeta^J \cong (2D^{JK}+4D^J)\zeta \quad (3a)$$

and

$$\zeta^K \cong (2D^{JK}+4D^K)\zeta. \quad (3b)$$

In any given degenerate vibrational state, the symmetry properties of the K-split levels are different, so that the sets of levels with upper and lower signs are associated with different transitions, $K'-K''=+1$ for one sign and -1 for the other. In addition to the standard terms in F given in eq (3), additional terms resulting from Coriolis-type interactions may occasionally be encountered when the energy differences between states of like over-all (vibrational and rotational) symmetry are small.

The energy terms resulting from inversion may conveniently be expressed in the form

$$E_{inv}(v,J,K)=E_v^i(v)\exp[b_v^i J(J+1)+(c_v^i-b_v^i)K^2+d_v^{iJ}J^2(J+1)^2+d_v^{iJK}J(J+1)K^2+d_v^{iK}K^4+\ \ldots \pm \tfrac{1}{2}f_n^i(A_1A_2), \quad (4)$$

where $E^0{}_{inv}$ is the splitting in the rotationless level, and the constants b^v, etc., represent the interaction of rotation and inversion. The term $f_n^i(A_1A_2)$ applies to the levels where states with over-all symmetry A_1 and A_2 form a nearly degenerate pair. There will then be an additional splitting term, depending on the value n of the K for which the degeneracy occurs. For $K=3$, in states of vibrational symmetry A (ground level, etc.), Nielsen and Dennison [16] have shown that

$$f_3^i(A_1A_2)=\beta_{3,v}(J-2)(J-1)J(J+1)(J+2)(J+3). \quad (4a)$$

For $K=2$, in one K-component of states of vibrational symmetry E,

$$f_2^i(A_1A_2)=\beta_{2,v}(J-1)J(J+1)(J+2) \quad (4b)$$

and for $K=1$, in the other K-component of states of vibrational symmetry E,

$$f_1^i(A_1A_2)=\beta_{1,v}J(J+1). \quad (4c)$$

Costain [17] has shown that the form (4) gives a much more rapidly convergent fit to the inversion of the ground state, for which data have been measured with very great accuracy [6], than does the representation in a simple power series in $J(J+1)$ and K^2. This is found to hold also for the vibrationally excited levels.

The values of the inversion constants for the ground state are $E_0^i=0.7934$ cm^{-1}; $b_0^i=-6.36996\times10^{-3}$, $c_0^i-b_0^i=8.88986\times10^{-3}$, $d_0^{iJ}=8.6922\times10^{-7}$, $d_0^{iJK}=-1.7845\times10^{-6}$, $d_0^{iK}=5.3075\times10^{-7}$, $\beta_{3,0}-1.17\times10^{-8}$ cm^{-1}. The resulting calculated values of $E_{inv}(0,J,K)$ are presented in table 1.

Spectral-line positions are given by subtracting lower-state energies from upper-state energies, both as given by eq (1) to (4). The selection rules governing the possible transitions are the well-known rules for the symmetric rotator, $\Delta J=\pm1,0$; $\Delta K=\pm1,0$, with additional restrictions upon the parity of the inversion state in eq (1) and the sign of the K-split state in eq (3), as imposed by the over-all symmetry. The bands analyzed are of the types whose rules are summarized in table 2. The notation s and a refers to the states whose wave functions are symmetric or antisymmetric with respect to the inversion plane; and the + or − signs under Δp refer to the actual algebraic sign in eq (1) corresponding to this symmetry. In perpendicular bands, only one of the two K-substates combines with the ground state, one sign being associated with transitions in the ${}^RP$-, ${}^RQ$-, and ${}^RR$-branches ($K'-K''=+1$) and the other with the ${}^PP$, ${}^PQ$, and ${}^PR$-branches ($K'-K''=-1$).

TABLE 1. *Calculated inversion splittings, 0^a-0^s (cm^{-1})*

J	$K=0\rightarrow$	1	2	3	4	5	6	7	8	9	10	11	12	13	14	15
0	0.793															
1	.783	0.790														
2	.764	.771	0.791													
3	.735	.742	.762	0.796												
4	.699	.705	.724	.757	0.805											
5	.656	.662	.680	.710	.756	0.818										
6	.608	.614	.630	.659	.700	.758	0.836									
7	.557	.562	.577	.601	.641	.694	.765	0.858								
8	.504	.508	.522	.553	.580	.627	.691	.775	0.885							
9	.450	.454	.466	.474	.518	.560	.617	.692	.789	0.917						
10	.398	.401	.412	.458	.457	.495	.544	.610	.696	.807	0.954					
11	.348	.351	.360	.327	.398	.432	.473	.532	.606	.703	.830	0.998				
12	.300	.303	.311	.404	.344	.372	.409	.459	.521	.605	.714	.857	1.048			
13	.256	.258	.265	.147	.294	.317	.349	.390	.444	.514	.606	.728	0.889	1.106		
14	.216	.218	.224	.432	.249	.268	.294	.329	.374	.433	.510	.611	.744	0.926	1.172	
15	.181	.182	.187	.080	.207	.224	.245	.274	.311	.360	.424	.507	.618	.767	0.969	1.247

TABLE 2. *Selection rules for* NH_3

Type	Δl	ΔP	ΔK	Sign in eq (3)	Example
∥, $a-s$	0	+←−	0		$\nu_1+\nu_2$, upper, ν_0=4,320 cm^{-1}.
∥, $s-a$	0	−←+	0		$\nu_1+\nu_2$, lower, ν_0=4,294 cm^{-1}.
⊥, $a-s$	1←0	−←−	±1	∓	$\nu_3+\nu_2$, lower, ν_0=4,417 cm^{-1}.
⊥, $s-a$	1←0	+←+	±1	∓	$\nu_3+\nu_2$, upper, ν_0=4,435 cm^{-1}.
⊥	2←0		±1	±	$2\nu_3^2$ ν_0=6,850 cm^{-1}.

The line strengths are given to first approximation by the familiar Hönl-London formulas [18], which apply rigorously to symmetric-top molecules in which there are no interactions between vibrations or between vibration and rotations. Such interactions are of nearly universal occurrence in molecules, but their magnitude is unpredictable, varies from band to band, and is frequently not large, so that the rigid line strengths are of essential value as guides to the relative intensities to be expected in all bands of a given molecule. The line strength may be written formally

$$S_{vr}(v',\ v'',\ J',\ J'',\ K',\ K'')=S_vH^0(J,\ K)g(J,\ K)F(v,\ J,\ K)\exp\left[-E''(J'',\ K'')/kT\right]/Q_r. \quad (5)$$

S_{vr} is the strength of each vibration-rotation line, where S_v is the total strength of all lines in the vibrational transition; $H^0(J,\ K)$ are the Hönl-London factors; $g(J,\ K)$ is the statistical weight; $F(v,\ J,\ K)$ is the correction factor for vibration-rotation interactions; $E''(J'',\ K'')$ is the ground-state energy, and Q_r is the rotational state-sum, $Q_r=\sum_{JK} ge^{-E''/KT}$.

For the ground levels (s, a) of NH_3, with three equivalent nuclei of spin 1/2,

$$g=\begin{cases} 4(2J+1) & \text{for } K=0,\ J \text{ even } (a) \text{ and } J \text{ odd } (s) \\ 0 & \text{for } K=0,\ J \text{ odd } (a) \text{ and } J \text{ even } (s) \\ 2(2J+1) & \text{for } K=1,\ 2,\ 4,\ 5,\ \ldots \\ 4(2J+1) & \text{for } K=3,\ 6,\ 9,\ \ldots . \end{cases}$$

The Hönl-London factors are

Branch	$K'-K''$	$J'-J''$	$H^0(J'',K'')$	
${}^QP$	0	−1	$(J^2-K^2)/J(2J+1)$	(5a)
${}^QQ$	0	0	$K^2/J(J+1)$	(5b)
${}^QR$	0	+1	$[(J+1)^2-K^2]/(J+1)(2J+1)$	(5c)
${}^PP$	−1	−1	$(J-1+K)(J+K)/4J(2J+1)$	(5d)
${}^PQ$	−1	0	$(J+1-K)(J+K)/4J(J+1)$	(5e)
${}^PR$	−1	+1	$(J+2-K)(J+1-K)/4(J+1)(2J+1)$	(5f)
${}^RP$	+1	−1	$(J-1-K)(J-K)/4J(2J+1)$	(5j)
${}^RQ$	+1	0	$(J+1+K)(J-K)/4J(J+1)$	(5k)
${}^RR$	+1	+1	$(J+2+K)(J+1+K)/4(J+1)(2J+1)$.	(5l)

In (5j), (5k), and (5l), when $K=0$, an additional factor 2 is required.

Using formulas (5), values of E'' calculated from the rotational constants to be derived and presented at a later point, and assuming $F=1$, values of S_{vr}/S_v have been calculated for $T=298°$ K. These are presented in table 3, as normalized to the value $S_v=10{,}000$.

The entries with $K''=0$ carry suffixes s or a to indicate which one of the inversion levels is present, and that the line is absent in the other band. The other entries apply to both a-s and s-a bands, except that in the calculation the energy difference between

the 0^s and 0^a states was ignored, so that the values given are averages; actually for *a-s* bands the strengths will be about 0.2 percent higher, and for *s-a*, 0.2 percent lower than tabulated.

When lines in an observed band are arranged as in table 3, by (J',K'), the derivation of molecular constants is facilitated. Rotational analyses are presented in tables of similar format. It will be noted that the strengths entered in table 3 range from a maximum of 236 down to 0.02, on the scale for which the total strength of lines in an inversion pair of bands is 10,000. It has not seemed necessary to extend the tables further, since only in exceptionally strong bands with excellent resolution will the weakest lines be observable. In most bands, however, lines down to $S_r=0.2$ should be observed if they can be resolved from stronger neighbors. In many of the parallel bands the lines with J' constant may not be fully resolved into their K-components, especially for low K.

The analysis of parallel bands presents no great difficulty. The Q-branches (which contain altogether 39.2 percent of the total band strength) can in general be recognized readily. They are never completely resolved; even when $(B'-B'')$ and $(C'-C'')$ are both large, there is considerable overlapping, and the weakest lines, those where $K<J$, are difficult to distinguish. The strongest Q-branch lines, as table 3 shows, are those with $K=J$, and these can usually be picked out, forming a regular series with $\nu\cong\nu_0+(B'-B'')J+(C'-C'')J^2$. (These remarks apply to each of the inversion-doubling bands; the two bands may overlap, but in many cases are widely separated.) The P- and R-branches may then be located, the K-substructure of each J-line, with the number of components increasing with J, forming when resolved, a characteristic pattern of lines with $\nu\cong\nu_{m,0}+aK^2$, and with the intensity of every third line enhanced. Arrangement of the lines of the three branches into tabular form should reveal constant combination differences

$$\Delta_1F''(J',K')={}^QR(J+1,K)-{}^QQ(J+1,K)={}^QQ(J,K)-{}^QP(J,K)=2(B_0-D_0^{JK}K^2)J-4D_0^JJ^3 \qquad (6)$$

or, when the Q-branch line is too weak to observe

$$\Delta_2F''(J',K')={}^QR(J,K)-{}^QP(J,K)=(4J+2)[B_0-D_0^{JK}K^2-2D_0^J(J^2+J+1)]. \qquad (6a)$$

In the analysis of perpendicular bands when observed under high-resolution conditions, it has been desirable to proceed rather differently from the manner usually reported in the literature, which applies when resolution is insufficient to separate the groups of lines constituting the ${}^PQ$- and ${}^RQ$-branches. With such incomplete resolution, only the mean position of all lines with common K, but varying J, is measured,

TABLE 3. *Rotational line strengths in* NH_3

The tabulated quantity is $10^4\ S_{vr}/S_v$, calculated by eq (5) for $T=298°$ K.

	Parallel bands			Perpendicular bands					
J'_K	${}^QP$	${}^QQ$	${}^QR$	${}^PP$	${}^PQ$	${}^PR$	${}^RP$	${}^RQ$	${}^RR$
0	62.0[s]			15.7					
1_0	102.0[a]		68.0[a]	19.5	23.6				
1_1	39.0	47.2		42.5			25.5[a]	93.0[s]	68.0[a]
2_0	115.2[s]		123.5[s]	19.5	32.5	7.87			
2_1	52.0	21.7	47.2	34.3	22.9		38.4[s]	125.7[a]	93.0[s]
2_2	34.3	91.6		112.5			3.25	21.7	47.2
3_0	104.2[a]		152.9[a]	17.0	34.1	12.99			
3_1	49.9	11.35	69.3	26.3	30.0	4.57	39.1[a]	134.3[s]	102.0[a]
3_2	42.1	48.0	45.7	80.4	39.4		4.98	28.4	43.3
3_3	53.7	236.2		60.8			1.75	18.0	68.6
4_0	81.1[s]		153.5[s]	12.35	29.9	14.61			
4_1	39.5	5.98	73.1	18.26	28.4	7.71	32.4[s]	117.3[a]	96.0[s]
4_2	36.5	25.2	61.7	53.2	48.3	5.62	4.94	26.9	36.5
4_3	60.8	124.1	78.7	38.7	15.63		2.61	22.1	54.0
4_4	19.35	125.0		56.8			1.90	27.6	157.5
5_0	54.7[a]		130.4[a]	8.09	21.3	13.28			
5_1	27.1	3.02	63.8	11.44	22.3	8.42	22.8[a]	89.2[s]	78.2[a]
5_2	26.1	12.74	58.9	32.1	41.8	9.20	3.87	21.1	28.0
5_3	48.1	62.6	98.1	22.7	17.74	1.737	2.45	19.1	39.3
5_4	20.2	63.1	31.3	32.6	11.57		2.67	31.3	110.4
5_5	13.0	115.7		95.1			0.504	9.86	78.2
6_0	32.9[s]		97.3[s]	4.84	15.09	10.30			
6_1	16.59	1.44	48.0	6.46	15.17	7.24	14.08[s]	59.1[a]	56.7[s]
6_2	16.18	6.06	46.4	17.64	29.8	9.50	2.59	14.37	19.2
6_3	31.4	29.8	85.4	12.19	14.05	2.69	1.795	13.65	26.1
6_4	14.61	30.0	35.8	17.15	12.10	1.052	2.35	24.8	71.2
6_5	12.47	55.0	23.1	49.6	16.06		0.664	10.31	49.3
6_6	16.42	192.6		36.2			.260	6.60	69.4
7_0	17.47[a]		63.8[a]	2.51	9.06	6.96			
7_1	8.79	0.648	31.8	3.30	9.09	5.25	7.66[a]	35.2[s]	36.4[a]
7_2	8.82	2.69	31.5	8.81	18.37	7.64	1.461	8.74	11.97
7_3	17.61	13.22	61.1	5.97	9.14	2.60	0.760	8.42	15.75
7_4	8.69	13.28	28.5	8.27	8.77	1.522	1.602	16.16	42.0
7_5	8.28	24.4	24.4	23.4	13.00	0.618	0.543	7.48	28.5
7_6	14.41	85.2	32.1	17.0	5.23		.318	5.35	39.6
7_7	4.86	73.2		25.4			.257	8.28	112.4

TABLE 3. *Rotational line strengths in* NH_3—Continued

	Parallel bands			Perpendicular bands					
J'_K	^QP	^QQ	^QR	^PP	^PQ	^PR	^RP	^RQ	^RR
8_0	8.41[a]	--------	37.5[a]	1.185	4.73	4.23	--------	--------	--------
8_1	4.21	0.263	19.04	1.526	4.85	3.30	3.73[a]	18.58[a]	21.12[a]
8_2	4.27	1.110	18.94	4.00	9.98	5.14	0.738	4.80	6.80
8_3	8.72	5.44	37.7	2.67	5.13	1.938	.582	4.67	8.64
8_4	4.44	5.48	18.60	3.64	5.20	1.364	.908	9.08	22.64
8_5	4.50	10.01	17.75	10.19	10.21	1.657	.342	4.44	15.12
8_6	8.72	35.0	30.8	7.32	4.59	0.348	.240	4.20	20.69
8_7	3.90	30.0	10.46	10.95	3.19	--------	.291	3.65	58.0
8_8	2.74	51.1	--------	34.5	--------	--------	.061	4.89	41.8
9_0	3.62[a]	--------	19.69[a]	0.507	2.25	2.23	--------	--------	--------
9_1	1.826	0.100	9.91	.641	2.31	1.83	1.634[a]	8.87[a]	10.93[a]
9_2	1.863	.421	10.05	1.651	4.82	2.99	0.333	2.20	3.40
9_3	3.85	2.07	20.50	1.085	2.53	1.206	.272	2.21	4.31
9_4	2.00	2.15	10.46	1.464	2.66	0.942	.444	4.49	11.10
9_5	2.09	3.80	10.56	4.05	5.53	1.373	.179	2.27	7.31
9_6	4.32	13.28	20.61	2.88	2.78	0.432	.139	2.28	9.89
9_7	2.16	11.34	9.23	4.42	2.60	.188	.202	4.42	27.45
9_8	2.08	19.58	6.39	12.73	3.68	--------	.064	1.97	19.59
9_8	2.83	66.3	--------	9.91	--------	--------	.029	1.376	28.75
10_0	1.419[a]	--------	9.35[a]	0.196	0.967	1.066	--------	--------	--------
10_1	0.715		4.69	.244	1.001	0.902	0.634[a]	3.80[a]	5.13[a]
10_2	.732	0.148	4.79	.621	2.100	1.531	.134	0.948	1.57
10_3	1.526	.725	9.91	.403	1.116	0.646	.113	.964	1.95
10_4	0.807	.729	5.17	.538	1.198	.540	.191	1.980	4.96
10_5	.862	1.281	5.40	1.466	2.578	.873	.081	1.025	3.10
10_6	1.832	4.62	11.17	1.038	1.375	.329	.067	1.065	4.32
10_7	0.978	3.96	5.60	1.505	1.490	.217	.108	2.191	11.88
10_8	1.005	7.07	5.21	4.51	2.700	.194	.0405	1.092	8.40
10_9	1.897	23.02	7.36	3.48	0.996	--------	.0264	1.049	12.39
10_{10}	0.695	19.93	--------	5.53	--------	--------	.0238	1.421	38.77
11_0	0.500[a]	----------	3.98[a]	0.069	0.379	0.460	----------	----------	----------
11_1	.253		2.01	.084	.390	.396	0.229[a]	1.48[a]	2.17[a]
11_2	.261	0.048	2.06	.213	.824	.693	.049	0.371	0.654
11_3	.546	.235	4.31	.136	.441	.304	.042	.377	.804
11_4	.291	.235	2.28	.180	.481	.265	.072	.785	2.02
11_5	.316	.429	2.44	.488	1.053	.460	<.02	.411	1.30
11_6	.689	1.488	5.22	.342	0.584	.192		.439	1.72
11_7	.380	1.274	2.77	.492	.642	.158		.929	4.69
11_8	.415	2.16	3.00	1.462	1.365	.203		.495	3.29
11_9	.875	7.36	5.41	1.120	0.668	.046		.505	5.00
11_{10}	.426	6.36	1.99	1.77	.504	----------		.954	14.21
11_{11}	.322	11.10	----------	5.83	----------	----------		.349	10.95
12_0	0.155[a]	----------	1.544[a]	<0.02	0.132	0.180	----------	----------	----------
12_1	.081		0.780		.137	.158	0.074[a]	0.529[a]	0.837[a]
12_2	.084		.804	.068	.281	.281	<.02	.131	.248
12_3	.178	0.070	1.686	.042	.149	.127		.134	.301
12_4	.095	.070	0.903	.056	.173	.116		.292	.749
12_5	.104	.128	.978	.148	.386	.207		.158	.478
12_6	.230	.441	2.136	.104	.210	.093		.161	.642
12_7	.130	.377	1.182	.147	.249	.079		.349	1.68
12_8	.147	.638	1.291	.433	.561	.131		.192	1.18
12_9	.368	2.17	2.738	.330	.308	.046		.208	1.69
12_{10}	.179	1.866	1.339	.519	.309	.022		.441	5.03
12_{11}	.171	3.26	1.008	1.69	.488	--------		.215	3.84
12_{12}	.282	11.68	--------	1.43	--------	--------		.161	6.05
13_0	0.044[a]	----------	0.542[a]		0.042	0.064	--------	--------	--------
13_1	.023		.278		.044	.057	0.022[a]	0.167[a]	0.292[a]
13_2	.024		.286		.094	.103		.042	.086
13_3	.051		.597		.051	.047		.043	.102
13_4	.029		.322		.056	.044		.092	.255
13_5	.031		.359	0.047	.127	.082		.049	.161
13_6	.070	0.120	.780	.032	.073	.039		.053	.210
13_7	.040	.103	.443	.047	.085	.034		.117	.560
13_8	.047	.174	.500	.119	.199	.064		.066	.388
13_9	.108	.587	1.254	.090	.115	.0267		.075	.552
13_{10}	.063	.505	0.616	.137	.131	.0195		.166	1.625
13_{11}	.071	.878	.586	.46	.273	.0195		.091	1.236
13_{12}	.147	3.39	.978	.38	.110	--------		.091	1.94
13_{13}	.058	2.87	----------	.65	--------	--------		.141	6.34
14_0		--------	0.173[a]				--------	--------	--------
14_1			.089					0.049[a]	0.087[a]
14_2			.093			0.0339			.024
14_3			.195						.032
14_4			.104					.026	.076
14_5			.115			.0290			.049
14_6			.258						.064
14_7			.147					.035	.169
14_8			.173			.0262			.117
14_9		0.146	.403						.165
14_{10}		.128	.234					.054	.481
14_{11}		.190	.263	0.107					.350
14_{12}	0.048	.783	.550	.086					.568
14_{13}		.723	.217	.15				.075	1.84
14_{14}		1.39	--------	.59				.029	1.54
15_{10}									0.121
15_{11}									.094
15_{12}		0.18							.143
15_{13}		.16							.456
15_{14}		.31		0.12					.40
15_{15}		1.27		.13					.74
16_{13}		0.028							0.083
16_{14}		.062							.069
16_{15}		.27							.116
16_{16}		.27							.63

and form a parabolic series around the band center. In NH_3, however, $(B'-B'')$ is in most bands so high that for each K, the ${}^RQ$ and ${}^PQ$ lines (each of which is in a series with $\nu=\nu_{Q0}+(B'-B'')J(J+1)+\ldots$) extend over several K-intervals, and the region of the band center is confusingly complex. A much simpler pattern is found in the band wings, containing the ${}^PP$- and ${}^RR$-branches, which are the stongest individual lines, and which may be arranged into J series with $K=J$, $K=J-1$, $K=J-n$, . . ., whose intensity falls off with increasing n.

From eq (3), and the selection rules neglecting the centrifugal-stretching terms, it may be shown that the frequencies of the ${}^RR(J''K'')$ and ${}^PP(J'',K'')$ lines are given by

$$\nu=\nu_0+(B''-C'')+2n(B''-C''+C\zeta)+n^2(B''-B'-C''+C')\pm J[2(C''-C'\zeta)\pm(B'-B'')-2n(B''-B'-C''+C')]+J^2(C'-C''). \quad (7)$$

Therefore, the mean spacing in the series of strongest lines with $n=0$ is $\sim 2(C_0-C_v\zeta)$. Since approximate values of $C_0\sim(6.2\ \mathrm{cm^{-1}})$ and ζ_v are known from previous work, the ${}^PP$ and ${}^RR$ series can usually be located, with tentative numberings. The identifications may then be corroborated by finding lines of the other branches with the same ground-state combination differences as found in the parallel bands and with intensities roughly paralleling the theoretical line strengths. For the combination differences in perpendicular bands, eq (6) applies, except that in the branches involved are ${}^RR-{}^RQ$, ${}^PR-{}^PQ$, etc.

3. Results

3.1. Molecular Constants

The NH_3 spectrum between 4,060 and 4,720 $\mathrm{cm^{-1}}$ contains over 800 resolved features, many of which are blends of lines whose separation is less 0.10 $\mathrm{cm^{-1}}$, the highest resolution obtained. Practically all the lines at frequencies above 4,250 $\mathrm{cm^{-1}}$, and a large proportion of the strong lines from 4,060 to 4,250 $\mathrm{cm^{-1}}$, have been analyzed into the inversion-doubled perpendicular bands $\nu_2+\nu_3$ and the weaker inversion-doubled parallel bands $\nu_1+\nu_2$. The analysis has yielded complete energy levels of $\nu_1+\nu_2$ up to $J=10$; and of $\nu_2+\nu_3$ up to $J=12$, in addition to some of the levels of higher J in both bands. The levels have been fitted to rotational-energy expressions of the forms of eq (3) and (4). The specific methods of deriving the constants and their values will be presented shortly. The line positions as calculated from the equations and constants are presented in tables 4 and 5, for the parallel and perpendicular bands, respectively. Following the calculated frequency (in $\mathrm{cm^{-1}}$) is tabulated the difference (in $10^{-2}\ \mathrm{cm^{-1}}$) between the observed frequency and that calculated. Suffixes are added to the difference when the observed feature is a blend, the suffix *a* designating a line principally due to the calculated line; *b*, a line of which about one-half the intensity is contributed by the calculated line; and *c*, a feature principally due to a line other than the one in question. It will be noted that the differences, except for the latter types of blends, and for the levels of highest J for which the calculation is relatively uncertain, are less than 0.1 $\mathrm{cm^{-1}}$, and average about 0.02 $\mathrm{cm^{-1}}$.

Representative spectra from 4,230 to 4,530 $\mathrm{cm^{-1}}$ are presented in figures 1 and 2. These were obtained at pressures of less than 1 cm in the 10-m cell. Some of the more prominent lines are indicated above the spectra. Below the spectra are plotted lines whose position is that of ν_{calc}, and whose height is proportional to

$$W=[(\nu/\nu_0)k(S^0_{vr}/S^0_v)\gamma^0]^{1/2}, \quad (8)$$

in which S^0_{vr}/S^0_v is the rigid rotational line strength (table 3), and k is an empirical factor to represent the relative strength of the perpendicular and parallel transitions, here taken as 100:15. The ν/ν_0 factor gives the small frequency dependence of line strength, ν_0 being taken as the mean band origins, 4,307 cm for $\nu_1+\nu_2$ and 4,426 cm for $\nu_2+\nu_3$. γ^0 is the collision half-width, whose evaluation and dependence upon (J,K) is discussed later. For nonoverlapping lines, eq (8) is a good representation of the equivalent width (integrated fractional absorption) [7], and hence the heights of the vertical lines

TABLE 4. *Calculated and observed frequencies in* $\nu_1+\nu_2$, NH_3

The first entry is $\nu_{\mathrm{calc}}(\mathrm{cm^{-1}})$; the second entry is $\nu_{\mathrm{obs}}-\nu_{\mathrm{calc}}$ $(10^{-2}\ \mathrm{cm^{-1}})$.

J'_K	p''	${}^QP$	${}^QQ$	${}^QR$
0	*s*	4300.17 03	----------	----------
1_0	*a*	4253.85 $\overline{08}^b$	----------	4313.47 $\overline{01}$
1_1	*s*	79.99 00	4319.75 03	----------
1_1	*a*	53.74 03^b	4293.49 08	----------
2_0	*s*	4259.32 00^b	----------	4358.66 01^a
2_1	*s*	59.39 $\overline{07}^b$	4318.98 $\overline{02}^a$	58.75 $\overline{09}^c$
2_1	*a*	33.68 $\overline{02}$	4293.24 07	32.99 01
2_2	*s*	59.60 $\overline{01}$	4319.23 01	----------
2_2	*a*	33.36 $\overline{01}$	4292.95 $\overline{03}^a$	----------
3_0	*a*	4213.62 $\overline{02}^b$	----------	4352.51 $\overline{01}^a$
3_1	*s*	38.45 $\overline{03}$	4317.83 02	77.43 $\overline{05}^b$
3_1	*a*	13.52 10^b	4292.87 11^c	52.43 07^b
3_2	*s*	38.66 $\overline{07}^a$	4318.07 $\overline{03}$	77.70 $\overline{03}$
3_2	*a*	13.20 00	4292.58 02^a	52.17 14^c
3_3	*s*	39.00 $\overline{04}^a$	4318.48 04^b	----------
3_3	*a*	12.66 $\overline{02}$	4292.09 04^a	----------
4_0	*s*	4217.20 $\overline{02}^b$	----------	4395.63 00^b
4_1	*s*	17.26 $\overline{08}^b$	4316.33 02^c	95.71 $\overline{08}^b$
4_1	*a*	4193.31 00	4292.34 ^{c}	71.69 $\overline{07}$
4_2	*s*	4217.44 $\overline{07}$	4316.56 01	95.97 00^b
4_2	*a*	4192.99 $\overline{02}$	4292.07 06^c	71.45 $\overline{07}$
4_3	*s*	4217.75 $\overline{03}^a$	4316.94 01^b	96.42 01
4_3	*a*	4192.46 $\overline{04}$	4291.60 10^b	71.04 01
4_4	*s*	4218.21 01	4317.51 01	----------
4_4	*a*	4191.68 $\overline{04}$	4290.92 05^b	----------
5_0	*a*	4173.16 $\overline{03}^b$	----------	4390.78 $\overline{05}^b$

See footnotes at end of table.

TABLE 4. *Calculated and observed frequencies in* $\nu_1+\nu_2$, NH_3—Continued

The first entry is ν_{calc}(cm^{-1}); the second entry is $\nu_{obs}-\nu_{calc}$ (10^{-2} cm^{-1}).

J'_K	p''	^QP	^QQ	^QR
5_1	*s*	95.80 $\overline{04}$	4314.48 [c]	4413.55 $\overline{07}$[b]
5_1	*a*	73.04 09[b]	4291.67 [c]	4390.70 03
5_2	*s*	95.96 $\overline{07}$[a]	4314.68 $\overline{03}$	4413.80 $\overline{04}$
5_2	*a*	72.74 $\overline{08}$	4291.42 00	4390.49 $\overline{04}$[c]
5_3	*s*	96.23 $\overline{04}$	4315.05 $\overline{02}$[b]	4414.24 02[b]
5_3	*a*	72.21 00	4290.98 $\overline{01}$[b]	4390.12 00[b]
5_4	*s*	96.64 $\overline{03}$	4315.59 $\overline{01}$	4414.88 00
5_4	*a*	71.44 $\overline{02}$	4290.33 $\overline{01}$	4389.57 $\overline{01}$
5_5	*s*	97.22 $\overline{02}$	4316.32 03[a]	----------
5_5	*a*	70.41 $\overline{04}$	4289.45 00	----------
6_0	*s*	4174.10 08[b]	----------	4430.89 12[b]
6_1	*s*	74.14 $\overline{04}$[b]	4312.30 [c]	30.97 $\overline{04}$[b]
6_1	*a*	52.75 $\overline{07}$[b]	4290.85 [c]	09.48 $\overline{02}$[b]
6_2	*s*	74.28 $\overline{10}$[b]	4312.49 [c]	31.22 $\overline{02}$[b]
6_2	*a*	52.44 $\overline{02}$[b]	4290.61 $\overline{09}$[c]	09.28 00
6_3	*s*	74.52 00	4312.84 04	31.66 02
6_3	*a*	51.91 $\overline{03}$	4290.18 04[b]	08.94 00[a]
6_4	*s*	74.87 $\overline{02}$	4313.34 $\overline{08}$[b]	32.28 02
6_4	*a*	51.17 $\overline{09}$	4289.57 00[a]	08.46 $\overline{02}$[c]
6_5	*s*	75.37 00	4314.02 $\overline{01}$	33.12 $\overline{08}$[c]
6_5	*a*	50.16 $\overline{08}$	4288.75 $\overline{01}$[b]	07.78 $\overline{05}$[a]
6_6	*s*	76.04 05	4314.92 11[a]	----------
6_6	*a*	48.86 $\overline{12}$	4287.67 $\overline{06}$[a]	----------
7_0	*a*	4132.51 01[b]	----------	4428.03 $\overline{01}$[b]
7_1	*s*	52.30 12[b]	4309.81 [c]	47.96 $\overline{22}$[b]
7_1	*a*	32.41 14[b]	4289.87	27.97 $\overline{05}$[c]
7_2	*s*	52.42 00[b]	4390.99 02	48.21 $\overline{03}$
7_2	*a*	32.11 04[b]	4289.63 $\overline{06}$[c]	27.80 $\overline{13}$[c]
7_3	*s*	52.64 04[b]	4310.31 06[c]	48.63 15
7_3	*a*	31.60 03[b]	4289.24 06	27.50 04
7_4	*s*	52.91 12	4310.77 $\overline{08}$[c]	49.24 $\overline{06}$
7_4	*a*	30.87 05[b]	4288.67 07[c]	27.07 $\overline{04}$
7_5	*s*	53.33 $\overline{06}$	4311.40 $\overline{19}$[b]	50.05 $\overline{03}$[c]
7_5	*a*	29.86 $\overline{10}$	4287.89 $\overline{02}$	26.48 $\overline{05}$
7_6	*s*	53.90 04	4312.23 09[a]	51.19 $\overline{10}$[b]
7_6	*a*	28.62 $\overline{10}$	4286.88 04[a]	25.69 $\overline{15}$[c]
7_7	*s*	54.67 03	4313.31 $\overline{05}$[b]	----------
7_7	*a*	27.04 $\overline{24}$	4285.60 $\overline{10}$	----------
8_0	*s*	4130.33 $\overline{07}$[b]	----------	4464.47 $\overline{17}$[b]
8_1	*s*	30.36 $\overline{10}$[b]	4307.05 $\overline{02}$[c]	64.55 $\overline{04}$[b]
8_1	*a*	12.06 $\overline{08}$	4288.70 [c]	46.15 $\overline{01}$[b]
8_2	*s*	30.44 $\overline{07}$[b]	4307.21 16[c]	64.79 $\overline{08}$[b]
8_2	*a*	11.77 $\overline{23}$[c]	4288.48 [c]	46.00 $\overline{14}$[b]
8_3	*s*	30.58 $\overline{07}$[b]	4307.50 $\overline{13}$[c]	65.19 $\overline{12}$
8_3	*a*	11.28 $\overline{17}$	4288.12 00	45.76 04
8_4	*s*	30.83 09[b]	4307.92 16	65.78 $\overline{24}$[c]
8_4	*a*	10.56 09	4287.58 03[c]	45.38 08
8_5	*s*	31.16 $\overline{09}$	4308.49 25	66.56 22
8_5	*a*	09.61 $\overline{09}$[b]	4286.87 05[a]	44.87 $\overline{07}$[c]
8_6	*s*	31.63 00[b]	4309.25 13	67.55 15
8_6	*a*	08.39 $\overline{19}$[b]	4285.93 $\overline{23}$[a]	44.19 $\overline{01}$[b]
8_7	*s*	32.27 $\overline{12}$[b]	4310.23 14[c]	68.87 10
8_7	*a*	06.86 $\overline{05}$	4284.74 $\overline{08}$[b]	43.29 $\overline{07}$
8_8	*s*	33.13 $\overline{02}$	4311.49 10[b]	----------
8_8	*a*	04.97 $\overline{17}$	4283.24 02[b]	----------
9_0	*a*	4091.78 17[b]	----------	4464.02 01[b]
9_1	*s*	4108.32 $\overline{12}$[b]	4304.03 [c]	80.72 $\overline{02}$[b]
9_1	*a*	4091.69 26[b]	4287.34 [c]	63.98 05[b]
9_2	*s*	4108.38 $\overline{18}$[b]	4304.18 [c]	80.95 22[b]
9_2	*a*	4091.40 $\overline{18}$	4287.14 [c]	63.86 17[b]
9_3	*s*	4108.51 $\overline{19}$[b]	4304.43 40[c]	81.35 $\overline{11}$[c]
9_3	*a*	4090.90 $\overline{08}$	4286.81 11[c]	63.64 $\overline{14}$[b]
9_4	*s*	4108.66 $\overline{04}$[b]	4304.81 $\overline{02}$[c]	81.90 21
9_4	*a*	4090.24 $\overline{15}$	4362.28 $\overline{15}$[c]	63.34 16[b]

TABLE 4. *Calculated and observed frequencies in* $\nu_1+\nu_2$, NH_3—Continued

The first entry is ν_{calc}(cm^{-1}); the second entry is $\nu_{obs}-\nu_{calc}$ (10^{-2} cm^{-1}).

J'_K	p''	^QP	^QQ	^QR
9_5	*s*	4108.90 $\overline{20}$[b]	4305.32 $\overline{02}$[c]	82.65 02
9_5	*a*	4089.32 $\overline{04}$[c]	4285.66 04[c]	62.92 $\overline{04}$[c]
9_6	*s*	4109.27 $\overline{25}$[b]	4306.01 $\overline{14}$	83.62 $\overline{46}$[c]
9_6	*a*	4088.14 $\overline{09}$[c]	4284.80 $\overline{14}$[b]	62.35 $\overline{13}$
9_7	*s*	4109.77 25	4306.89 14[a]	4484.83 05
9_7	*a*	4086.68 05	4283.71 09[b]	61.59 07[c]
9_8	*s*	4110.46 19[b]	4308.02 19	86.39 13
9_8	*a*	4084.87 $\overline{18}$	4282.33 $\overline{07}$[b]	60.60 $\overline{15}$[b]
9_9	*s*	4111.41 03[b]	4309.48 $\overline{16}$	----------
9_9	*a*	4082.66 01	4280.61 $\overline{05}$[b]	----------
10_0	*s*	4086.25 05[c]	----------	4496.41 23[b]
10_1	*s*	86.26 $\overline{04}$[c]	4300.78	96.48 16[b]
10_1	*a*	71.31 $\overline{11}$[b]	4285.78	81.46 00[c]
10_2	*s*	86.29 01[c]	4300.91	96.70 $\overline{06}$[b]
10_2	*a*	71.04 16[b]	4285.61	81.34 12[c]
10_3	*s*	86.27 03[c]	4301.09 [c]	97.04 $\overline{04}$[c]
10_3	*a*	70.65 $\overline{05}$[c]	4285.35 [c]	81.25 $\overline{08}$
10_4	*s*	86.46 $\overline{16}$[c]	4301.17 16[c]	97.62 [c]
10_4	*a*	69.91	4284.86 [c]	80.94 $\overline{24}$[b]
10_5	*s*	86.63 $\overline{10}$[b]	4301.93 07[c]	98.34 34[b]
10_5	*a*	69.02 $\overline{24}$	4284.26 [c]	80.60 10[b]
10_6	*s*	86.88 $\overline{15}$[b]	4302.53 10	99.27 $\overline{10}$
10_6	*a*	67.90 $\overline{15}$	4283.48 $\overline{22}$[c]	80.14 $\overline{04}$
10_7	*s*	87.24 06	4303.32 $\overline{08}$	4500.43 $\overline{15}$
10_7	*a*	66.49 $\overline{27}$[c]	4282.48 $\overline{22}$[b]	4479.52 $\overline{13}$
10_8	*s*	87.76. 05[c]	4304.32 $\overline{44}$[c]	4501.88 $\overline{29}$[c]
10_8	*a*	64.86 $\overline{21}$[c]	4281.24 10[b]	4478.70 $\overline{22}$[c]
10_9	*s*	88.50 $\overline{01}$	4305.61 05	4503.67 05
10_9	*a*	62.68 $\overline{12}$	4279.68 $\overline{03}$[b]	4477.63 $\overline{09}$
10_{10}	*s*	89.53 $\overline{25}$[c]	4307.26 11[a]	----------
10_{10}	*a*	60.11 $\overline{39}$[c]	4277.72 02	----------
11_0	*a*	4051.02 $\overline{24}$	----------	4498.51 $\overline{17}$[b]
11_3	*s*	64.27	4297.63	4512.45 [c]
11_3	*a*	50.15	83.57	4498.26 08[b]
11_6	*s*	64.41 24[c]	98.78 $\overline{16}$	4514.44 $\overline{49}$
11_6	*a*	47.75 17	82.04	4497.62 [c]
11_7	*s*	64.71 $\overline{05}$[c]	99.54 [c]	4515.62 [c]
11_7	*a*	46.50 25	81.24 10[b]	4497.24 [c]
11_8	*s*	65.08 [c]	4300.43 24	4516.99 [c]
11_8	*a*	44.68 [c]	4279.94 [c]	4496.41 23[c]
11_9	*s*	65.61 $\overline{20}$	4301.56 07	4518.67 [c]
11_9	*a*	42.81 01[c]	4278.65 30	4495.66 19
11_{10}	*s*	66.38 [c]	4303.00 00[b]	4520.73
11_{10}	*a*	40.30	4276.80 08[c]	4494.41 18
11_{11}	*s*	67.50 [c]	4304.87 $\overline{04}$[b]	----------
11_{11}	*a*	37.34	4274.57 $\overline{22}$[b]	----------
12_9	*s*	----------	4297.52 48	4533.47 56
12_9	*a*	----------	77.36 $\overline{24}$	13.20 [c]
12_{10}	*s*	----------	98.67 $\overline{05}$[b]	35.30 23
12_{10}	*a*	----------	75.67 $\overline{03}$[c]	12.17 [c]
12_{11}	*s*	----------	4300.19 $\overline{22}$	37.56 [c]
12_{11}	*a*	----------	4273.67 24	10.90
12_{12}	*s*	----------	4302.28 $\overline{28}$	----------
12_{12}	*a*	----------	4271.28 14	----------
13_{12}	*s*	----------	4297.23 $\begin{cases}\overline{220}\\206\end{cases}$	4554.20 $\begin{cases}\overline{220}\\210\end{cases}$
13_{12}	*a*	----------	70.33 $\overline{07}$[c]	27.14
13_{13}	*s*	----------	99.71 $\overline{42}$	----------
13_{13}	*a*	----------	67.99 $\overline{16}$[b]	----------

[a] Blend, principally due to calculated line.
[b] Blend, approximately one-half due to calculated line.
[c] Blend, principally due to other line.

TABLE 5. *Calculated and observed frequencies in* $\nu_2+\nu_3$, NH_3

The first entry is ν_{calc} (cm^{-1}); the second entry is $\nu_{obs}-\nu_{calc}$ (10^{-2} cm^{-1}).

J'_K	p''	^PP	^PQ	^PR	^RP	^RQ	^RR
0	*s*	4400.79 $\overline{07}$[b]	----------	----------	----------	----------	----------
0	*a*	18.50 00	----------	----------	----------	----------	----------
1_0	*s*	4380.66 $\overline{06}$	4420.42 $\overline{06}$	----------	----------	----------	----------
1_0	*a*	98.10 05	37.84 09	----------	----------	----------	----------
1_1	*s*	4388.53 $\overline{03}$	----------	----------	----------	4412.54 $\overline{03}$	----------
1_1	*a*	4406.20 04	----------	----------	4390.42 03	----------	4450.04 $\overline{02}$[b]
2_0	*s*	4360.18 00	4419.77 $\overline{01}$	4459.54 $\overline{02}$	----------	----------	----------
2_0	*a*	77.35 03[b]	36.92 02	76.67 $\overline{01}$	----------	----------	----------
2_1	*s*	68.08 $\overline{02}$	27.70 $\overline{03}$	----------	4352.31 00[b]	----------	4451.66 04
2_1	*a*	85.39 07[b]	44.98 00	----------	----------	4429.24 $\overline{03}$	----------
2_2	*s*	76.04 01	----------	----------	44.60 $\overline{01}$	04.19 $\overline{03}$	43.96 $\overline{05}$
2_2	*a*	93.81 02	----------	----------	62.24 $\overline{06}$	21.81 $\overline{03}$	61.56 $\overline{04}$
3_0	*s*	4339.48 01	4418.86 $\overline{02}$	4478.45 03	----------	----------	----------
3_0	*a*	56.13.05	35.47 02	95.04 02[c]	----------	----------	----------
3_1	*s*	47.36 03	26.78 $\overline{02}$	86.40 $\overline{03}$	----------	4411.10 00	----------
3_1	*a*	64.14 03	43.52 02	4503.11 $\overline{00}$	4348.38 03	----------	4487.27 $\overline{03}$
3_2	*s*	55.31 01	34.78 03	----------	23.93 06[c]	03.32 00	62.91 $\overline{01}$
3_2	*a*	72.52 03	51.96 04	----------	41.04 01	20.38 $\overline{02}$	79.95 $\overline{01}$
3_3	*s*	63.37 00	----------	----------	16.20 15[c]	4395.61 02	55.23 $\overline{01}$
3_3	*a*	81.25 06	----------	----------	33.96 04	4413.34 $\overline{04}$	72.93 00
4_0	*s*	4318.56 $\overline{04}$[c]	4417.64 $\overline{03}$	4497.02 $\overline{02}$	----------	----------	----------
4_0	*a*	34.54 03	33.56 00[a]	4512.91 00[c]	----------	----------	----------
4_1	*s*	26.42 00	25.54 00	04.96 $\overline{02}$	4310.67 04[c]	----------	4489.10 04
4_1	*a*	42.51 07	41.59 06[b]	20.97 04	----------	4425.99 $\overline{01}$	----------
4_2	*s*	34.33 06	33.52 04	13.00 $\overline{11}$[c]	03.07 $\overline{07}$	02.15 $\overline{03}$	81.53 $\overline{07}$
4_2	*a*	50.87 $\overline{03}$	50.01 01[b]	29.47 $\overline{02}$	19.48 00	18.51 $\overline{04}$	97.85 00
4_3	*s*	42.36.04	41.66 $\overline{01}$	----------	4295.38 00	4394.50 00	73.91 $\overline{02}$
4_3	*a*	59.55 06	58.80 07	----------	4312.38 $\overline{06}$	4411.46 $\overline{02}$	90.84 $\overline{02}$
4_4	*s*	50.47 05	----------	----------	4287.66 $\overline{04}$[c]	4386.86 $\overline{01}$	66.33 $\overline{02}$
4_4	*a*	68.63 02	----------	----------	4305.57 04	4404.72 $\overline{04}$[b]	84.15 $\overline{03}$
5_0	*s*	4297.43 07[b]	4416.11 04[b]	4515.18 01[b]	----------	----------	----------
5_0	*a*	4312.58 05	31.21 03	30.24 $\overline{03}$	----------	----------	----------
5_1	*s*	05.26 04	23.99 $\overline{04}$	23.11 $\overline{03}$	----------	4408.48 00	----------
5_1	*a*	20.53 03	39.20.01	38.28 04	4304.79 03	----------	4522.42 01
5_2	*s*	13.18.10	32.00 $\overline{01}$	31.19 $\overline{02}$	4282.00 00	00.68 $\overline{04}$	4499.75 $\overline{04}$
5_2	*a*	28.79.05	47.55 03	46.70 06[b]	97.56 $\overline{06}$	16.19.$\overline{04}$[b]	4515.22 $\overline{03}$
5_3	*s*	21.15 03	40.09 02	39.38 01	74.34 01	4393.07 08[a]	4492.18 00
5_3	*a*	37.45 03[c]	56.34 07	55.58 $\overline{03}$	90.49 $\overline{09}$[c]	4409.15 07	4508.23 $\overline{07}$[b]
5_4	*s*	29.23 03	48.33 02	----------	66.66 04	4385.48 $\overline{02}$[b]	4484.67 00
5_4	*a*	46.46 02	65.50 04	----------	83.65.15[c]	4402.41 03	4501.56 03
5_5	*s*	37.36 12[a]	----------	----------	58.93 $\overline{06}$	4377.87 $\overline{06}$	4477.16 $\overline{02}$
5_5	*a*	55.84 07	----------	----------	77.09 $\overline{21}$[c]	95.97 00[a]	95.21 $\overline{11}$
6_0	*s*	4276.10 04	4414.26 00	4532.93 $\overline{14}$[c]	----------	----------	----------
6_0	*a*	90.32 00[c]	28.42 01	47.05 01	----------	----------	----------
6_1	*s*	83.90 $\overline{10}$[c]	22.12 $\overline{02}$	40.84 $\overline{02}$	4268.18 06	----------	4524.97 03[b]
6_1	*a*	98.22 06	36.39 03	55.06 01	----------	4420.99 00	----------
6_2	*s*	91.70 00[b]	30.02 08	48.84 $\overline{01}$	60.74 $\overline{19}$	4398.90 $\overline{14}$	17.57 $\overline{23}$
6_2	*a*	4306.53 08[a]	44.79 01	63.55 $\overline{04}$	75.34 $\overline{02}$	4413.44 04	32.07 $\overline{01}$
6_3	*s*	4299.73 01	38.20 $\overline{03}$	57.14 04	53.12 $\overline{02}$	4391.34 06	10.06 $\overline{01}$
6_3	*a*	4315.03 00[c]	53.44 20	72.32 03	68.26 $\overline{02}$	4406.42 01	25.10 $\overline{10}$[b]
6_4	*s*	07.79 02	46.44 $\overline{06}$	65.54 $\overline{01}$	45.48 01	4383.80 04[a]	02.62 03
6_4	*a*	23.97 02[a]	62.54 $\overline{01}$	81.58 $\overline{03}$	61.42 01	99.69 03[a]	18.45 04
6_5	*s*	15.94 01	54.82 02	----------	37.79 $\overline{12}$[c]	76.26 02	4495.20 04
6_5	*a*	33.28 01	72.09 01	----------	54.83.$\overline{07}$[b]	93.24 03	4512.12 00
6_6	*s*	24.14 06	----------	----------	30.00 $\overline{15}$[c]	68.65 $\overline{00}$[c]	4487.75 01
6_6	*a*	43.02 02	----------	----------	45.49 00[b]	87.07 $\overline{04}$	4506.11 01
7_0	*s*	4254.58 $\overline{04}$	4412.08 00	4550.24 $\overline{02}$	----------	----------	----------
7_0	*a*	67.77 06	25.22 00	63.32 $\overline{08}$[b]	----------	----------	----------
7_1	*s*	62.34 01	19.92 $\overline{02}$	58.13 05[b]	----------	4404.62 06	----------
7_1	*a*	75.63 01	33.15 05[b]	71.32 00	4259.95 $\overline{01}$	----------	4555.47 $\overline{05}$

See footnotes at end of table.

473722—58——2

TABLE 5. *Calculated and observed frequencies in* $\nu_2+\nu_3$, NH_3—Continued

The first entry is ν_{calc} (cm^{-1}); the second entry is $\nu_{obs}-\nu_{calc}$ (10^{-2} cm^{-1}).

J'_K	p''	^PP	^PQ	^PR	^RP	^RQ	^RR
7_2	s	70.28 $\overline{02}$	27.97 05	66.29 $\overline{07}$	39.21 22	4396.81 20	34.96 11[b]
7_2	a	83.71 09[b]	41.35 04	79.61 03	52.85 $\overline{06}$[c]	4410.31 01	48.41 00
7_3	s	78.11 01[b]	35.97 $\overline{01}$	74.43 $\overline{04}$	31.72 00	4389.30 01	27.52 07[b]
7_3	a	92.31 $\overline{18}$[c]	50.11 $\overline{09}$[c]	88.51 $\overline{14}$	45.78 $\overline{01}$[a]	4403.30 02[c]	41.46 00
7_4	s	4286.15 02	4444.22 $\overline{04}$	4582.87 $\overline{06}$[b]	4224.14 03	4381.84 06	4520.16 04
7_4	a	4301.15 01	59.15 $\overline{01}$	97.74 $\overline{04}$	38.44 $\overline{02}$[c]	96.57 06	34.83 01
7_5	s	4294.28 $\overline{02}$	52.61 $\overline{03}$	91.49 $\overline{05}$	16.51 05[c]	74.37 09	12.83 08
7_5	a	4310.35 02[b]	68.61 $\overline{01}$	4607.42 $\overline{04}$[b]	32.32 03	90.12 00[b]	28.53 02
7_6	s	02.47 $\overline{07}$	61.10 00	----------	08.78 12	66.85 $\overline{04}$	05.50 06
7_6	a	19.99 $\overline{01}$	78.54 $\overline{06}$[c]	----------	25.94 15	83.94 $\overline{10}$[c]	22.53 04
7_7	s	10.69 $\overline{02}$[b]	----------	----------	00.88 09	59.21 $\overline{04}$	4498.09 04
7_7	a	30.06 $\overline{02}$	----------	----------	19.79 04	78.05 $\overline{08}$	4516.85 $\overline{09}$
8_0	s	4232.90 00	4409.59 $\overline{09}$[b]	4567.09 $\overline{02}$	----------	----------	----------
8_0	a	45.00 $\overline{02}$	21.64 04	79.04 00	----------	----------	----------
8_1	s	40.61 03	17.38 $\overline{06}$	74.96 $\overline{06}$	4224.97 $\overline{11}$	----------	4559.12 $\overline{10}$
8_1	a	52.81 $\overline{02}$[b]	29.53 $\overline{01}$	87.05 02	----------	4414.37 $\overline{11}$[a]	----------
8_2	s	48.20 $\overline{08}$	25.12 $\overline{10}$	82.81 $\overline{00}$[b]	17.72 00[c]	4394.41 09[c]	51.91 00
8_2	a	61.13 04[a]	37.96 $\overline{03}$	95.60 $\overline{03}$	30.15 10[a]	4406.79 03	64.24 $\overline{08}$
8_3	s	56.31 $\overline{05}$	33.40 00[c]	91.26 $\overline{04}$	10.19 04	4386.96 $\overline{11}$[c]	44.54 $\overline{05}$[b]
8_3	a	69.35 $\overline{17}$[b]	46.37 01[c]	4604.17 $\overline{12}$	23.09 03	99.80 $\overline{08}$[c]	57.32 $\overline{02}$
8_4	s	64.31 04	41.64 00[c]	4599.71 $\overline{01}$	02.64 05	79.55 07	37.24 $\overline{01}$
8_4	a	78.12 $\overline{02}$[b]	55.37 $\overline{15}$[c]	4613.38 $\overline{08}$	16.26 12[b]	93.10 07[c]	50.73. $\overline{01}$
8_5	s	72.42 $\overline{07}$	50.04 $\overline{02}$[c]	08.36 $\overline{05}$	4195.11 $\overline{01}$	72.20 02	30.05 $\overline{04}$
8_5	a	87.19 01	64.73 $\overline{02}$[a]	22.99 $\overline{02}$	4209.62 03	86.64 06	44.44 05[b]
8_6	s	80.60 $\overline{04}$[b]	58.57 $\overline{06}$	17.20 $\overline{16}$[c]	4187.45 03	64.77 07	22.84 03
8_6	a	96.69 $\overline{01}$	74.57 00	33.12 $\overline{02}$	4203.20 $\overline{06}$	80.46 04	38.46 02
8_7	s	88.83 $\overline{09}$[b]	67.19 $\overline{02}$	----------	4179.64 $\overline{03}$	57.25 07	15.58 $\overline{03}$
8_7	a	4306.62 $\overline{01}$[b]	84.89 10	----------	96.99 $\overline{04}$	74.54 04	32.79 00
8_8	s	4297.05 $\overline{01}$	----------	----------	71.60 $\overline{18}$[c]	49.56 06	08.20 $\overline{04}$[b]
8_8	a	4317.02 $\overline{07}$[b]	----------	----------	91.01 04	68.89 03	27.45 $\overline{01}$
9_0	s	4211.06 $\overline{04}$	4406.76 $\overline{03}$	4583.45 $\overline{05}$	----------	----------	----------
9_0	a	22.05 $\overline{11}$	17.71 $\overline{08}$[c]	94.35 $\overline{01}$[b]	----------	----------	----------
9_1	s	18.72 $\overline{01}$	14.52 $\overline{07}$	91.29 $\overline{07}$[b]	----------	4399.47 05	----------
9_1	a	29.81 04	25.55 $\overline{01}$[c]	4602 26 03	4214.24 $\overline{17}$	----------	4586.48 $\overline{13}$
9_2	s	26.78 $\overline{09}$	22.70 $\overline{04}$	4599.61 $\overline{06}$	4195.98 $\overline{09}$[c]	91.69 $\overline{06}$[b]	68.38 00
9_2	a	37.55 12	33.45 $\overline{05}$[b]	4610.29 10	4207.28 $\overline{21}$	4402.93 $\overline{10}$	79.57 $\overline{09}$
9_3	s	4234.34 $\overline{04}$	4430.49 02	4607.58 $\overline{12}$[b]	4188.51 03	4384.31 $\overline{03}$	4561.08 $\overline{04}$
9_3	a	46.19 $\overline{12}$	42.27 $\overline{05}$	19.29 $\overline{08}$	4200.24 $\overline{07}$	95.97 00[c]	72.70 $\overline{06}$
9_4	s	42.32 $\overline{13}$	38.73 $\overline{05}$	16.06 $\overline{05}$	4181.06 $\overline{03}$	77.00 $\overline{02}$	53.90 $\overline{03}$[b]
9_4	a	54.83 $\overline{07}$	51.17 04[b]	28.43 $\overline{06}$	93.39 $\overline{08}$[c]	89.28 03[b]	66.12 $\overline{01}$
9_5	s	50.40 $\overline{06}$	47.13 $\overline{07}$	24.75 $\overline{08}$	73.57 $\overline{29}$	69.71 $\overline{07}$	46.80 $\overline{04}$
9_5	a	63.82 $\overline{02}$	60.48 $\overline{03}$	38.02 $\overline{04}$	86.76 $\overline{01}$	82.84 $\overline{05}$	59.86 $\overline{02}$
9_6	s	58.57 $\overline{10}$	55.68 $\overline{07}$	33.64 $\overline{09}$	65.99 01	62.40 $\overline{03}$	39.73 00
9_6	a	73.18 $\overline{09}$	70.22 $\overline{05}$	48.10 $\overline{09}$[b]	80.30 06	76.65 $\overline{01}$	53.91 $\overline{04}$[b]
9_7	s	66.78 $\overline{08}$	64.34 $\overline{04}$[b]	42.70 00	58.28 01	55.02 08	32.63 03
9_7	a	82.94 02	80.41 04	58.67 01[b]	74.06 12[c]	70.72 02	48.26 03
9_8	s	75.03 $\overline{06}$[a]	73.09 $\overline{04}$[b]	----------	50.34 05	47.45 01[c]	25.42 03
9_8	a	93.18 $\overline{08}$	91.13 $\overline{06}$	----------	67.98 03[c]	65.02 00	42.90 00
9_9	s	83.26 00	----------	----------	42.11	39.67 $\overline{07}$	18.03 $\overline{05}$
9_9	a	4303.95 $\overline{07}$	----------	----------	62.16	59.62 $\overline{01}$[c]	37.89 $\overline{03}$
10_0	s	4189.10 $\overline{13}$	4403.62 $\overline{30}$[c]	4599.33 $\overline{09}$	----------	----------	----------
10_0	a	98.95 19	13.43 05[c]	4609.08 02	----------	----------	----------
10_1	s	96.71 $\overline{10}$[c]	11.34 10[c]	07.13 $\overline{05}$	4181.22 $\overline{01}$	----------	4591.38 $\overline{16}$[b]
10_1	a	4206.64 02	21.21 09[c]	16.95 09[b]	----------	4406.32 $\overline{11}$[c]	----------
10_2	s	03.95 $\overline{10}$	18.78 06[c]	14.70 02[b]	74.14 04[c]	4388.66 14	84.37 $\overline{05}$
10_2	a	15.08 00	29.77 14	25.67 04	83.26 $\overline{17}$	98.73 03[c]	94.38 $\overline{04}$[b]
10_3	s	12.24 $\overline{06}$	27.26 05	23.40 $\overline{02}$	66.74 $\overline{12}$	81.36 $\overline{05}$[c]	77.15 $\overline{11}$
10_3	a	22.86 04[b]	37.81 12[c]	33.89 $\overline{05}$	77.29 $\overline{17}$	91.86 $\overline{11}$[b]	87.60 $\overline{11}$
10_4	s	20.19 $\overline{02}$	35.49 00[c]	31.90 $\overline{06}$	59.35 $\overline{14}$	74.14 $\overline{08}$	70.08 $\overline{12}$
10_4	a	31.40 $\overline{02}$[b]	46.63 $\overline{01}$[b]	42.97 $\overline{02}$	70.41 07[c]	85.13 33[c]	81.02 $\overline{05}$

See footnotes at end of table.

TABLE 5. *Calculated and observed frequencies in* $\nu_2+\nu_3$, NH_3—Continued

The first entry is ν_{calc} (cm^{-1}); the second entry is $\nu_{obs}-\nu_{calc}$ (10^{-2} cm^{-1}).

J'_K	p''	^PP	^PQ	^PR	^RP	^RQ	^RR
10_5	s	28.25 $\overline{14}$	43.90 03[c]	40.64 $\overline{08}$	51.95 $\overline{07}$[c]	66.97 $\overline{07}$[c]	63.11 $\overline{11}$
10_5	a	40.25 $\overline{03}$	55.83 01	52.49 $\overline{03}$	63.75 $\overline{31}$	78.70 $\overline{06}$	74.78 $\overline{02}$
10_6	s	36.39 $\overline{09}$	52.47 $\overline{11}$[c]	49.58 $\overline{05}$	44.45 11[c]	59.75 $\overline{11}$[c]	56.16 $\overline{10}$
10_6	a	49.48 $\overline{07}$	65.48 $\overline{18}$	62.51 $\overline{01}$	57.28 19[c]	72.51 01[c]	68.95 $\overline{12}$
10_7	s	44.62 $\overline{12}$	61.18 $\overline{08}$[b]	58.73 $\overline{05}$[b]	36.94	52.49 01[c]	49.23 $\overline{05}$
10_7	a	59.10 00	75.57 00	73.03 01	50.97	66.55 02	63.21 03[b]
10_8	s	52.85 $\overline{06}$[b]	69.98 01	68.05 $\overline{01}$	29.02	45.10 01	42.21 02
10_8	a	69.13 05[b]	86.14 07	84.09 07	44.83	60.82 03	57.86 03
10_9	s	4261.11 06[b]	4478.84 20	----------	4120.92	4337.48 00[c]	4535.04 03[b]
10_9	a	79.65 00	97.25 $\overline{25}$[c]	----------	38.88	55.35 00[c]	52.82 02
10_{10}	s	69.32 16	----------	----------	----------	29.50 05	27.56 03[b]
10_{10}	a	90.77 $\overline{25}$[a]	----------	----------	----------	50.10 02	48.05 07
11_0	s	4167.03 $\overline{19}$	4400.16 $\overline{01}$	4614.68 04[b]	----------	----------	----------
11_0	a	75.76 05	08.84 10[c]	23.32 06[c]	----------	----------	----------
11_1	s	74.58 [c]	07.82 $\overline{09}$[c]	22.44 08[b]	----------	4393.02 13[c]	----------
11_1	a	83.39 13	16.57 23	31.14 14	4168.00 $\overline{27}$	----------	4615.49 $\overline{23}$
11_2	s	82.92 $\overline{25}$	16.27 $\overline{12}$[c]	31.09 $\overline{07}$	52.19 [c]	85.32 14[c]	4599.84 $\overline{14}$[b]
11_2	a	90.59 $\overline{27}$	24.02 $\overline{07}$[c]	38.70 00[b]	61.16 16	94.24 26[c]	4608.72 $\overline{05}$
11_3	s	90.02 $\overline{09}$	23.68 27[c]	38.69 01[b]	44.86 $\overline{30}$	78.10 $\overline{29}$[c]	4592.72 $\overline{19}$
11_3	a	99.43 15	33.03 17[c]	47.98 03[b]	54.17 [c]	87.35 06	4601.92 $\overline{06}$
11_4	s	97.95 $\overline{26}$	31.93 06[c]	47.23 $\overline{02}$	37.55 $\overline{28}$	70.96 $\overline{22}$	4585.74 $\overline{19}$
11_4	a	4207.89 $\overline{31}$	41.80 [c]	57.03 $\overline{10}$	47.35 $\overline{34}$	80.70 [c]	95.43 $\overline{08}$
11_5	s	05.94. $\overline{03}$	40.31 $\overline{20}$[c]	55.96 00	30.22 [c]	63.88 $\overline{15}$	78.89 $\overline{33}$
11_5	a	16.71 47[c]	50.90 31[c]	66.48. 31	40.69. $\overline{18}$	74.29 [c]	89.24 $\overline{09}$
11_6	s	14.07 00[b]	48.89 $\overline{11}$[c]	64.97 $\overline{01}$	----------	56.08 $\overline{37}$[b]	72.10 $\overline{33}$
11_6	a	26.14 $\overline{05}$	60.43 02[c]	76.42 11	----------	68.11 $\overline{05}$[c]	83.34 $\overline{09}$[b]
11_7	s	22.29 $\overline{03}$	57.64. $\overline{01}$	74.20 $\overline{02}$	----------	49.68 $\overline{35}$	65.33 $\overline{39}$
11_7	a	35.65. 08	70.39 19	86.87 18	----------	62.14 $\overline{26}$	77.73 $\overline{02}$[b]
11_8	s	30.57 07	66.51 25[b]	83.62 14	----------	42.44 $\overline{47}$	58.52 $\overline{34}$[b]
11_8	a	44.98 32	80.82 35[b]	97.83 39	----------	56.38. 05[b]	72.38 $\overline{03}$
11_9	s	38.83 60[b]	75.45 58	93.18 49[b]	----------	35.06 $\overline{15}$	51.60 $\overline{15}$
11_9	a	55.26 34	91.77 41[c]	4709.37 35	----------	50.86 04[c]	67.33 $\overline{01}$
11_{10}	s	47.05 $\overline{20}$	84.42 [c]	----------	----------	27.31 13	44.42 07[b]
11_{10}	a	66.07 03	4503.30 $\overline{19}$	----------	----------	45.57. $\overline{10}$[b]	62.57 04
11_{11}	s	55.21 $\overline{21}$	----------	----------	----------	19.19 05[c]	36.93 03
11_{11}	a	77.46 $\overline{58}$	----------	----------	----------	40.57 $\overline{16}$	58.17 01[a]
12_0	s	----------	4396.37 [c]	4629.50 01	----------	----------	----------
12_0	a	----------	4403.97 [c]	37.06 04[a]	----------	----------	----------
12_1	s	----------	03.98 [c]	37.22 10	4137.05 $\overline{37}$	----------	4621 62 $\overline{61}$
12_1	a	----------	11.65 $\overline{01}$	44.83 29	----------	4397.01 37	----------
12_2	s	4158.99 22[c]	10.91 [c]	44.25 29	----------	81.67 [c]	14.80 $\overline{08}$[c]
12_2	a	68.85 $\overline{11}$[c]	20.50 18	53.93 26	----------	89.48 [c]	22.57 20
12_3	s	----------	4419.76 [c]	4653.43 17	----------	4374.52 [c]	4607.77 $\overline{31}$[c]
12_3	a	----------	27.95 [c]	61.55 54[a]	----------	82.63 [c]	15.82 00
12_4	s	----------	27.97 [c]	61.95 14[a]	----------	67.49 $\overline{08}$	00.90 $\overline{55}$[b]
12_4	a	----------	36.62 [c]	70.52 38[b]	----------	76.02 $\overline{17}$	09.37 $\overline{13}$
12_5	s	4183.54 09	36.38 [c]	70.74 16	----------	60.52 [c]	4594.18 $\overline{30}$[c]
12_5	a	92.88 [c]	45.65 [c]	79.94 38	----------	69.64 00[c]	4603.24 $\overline{10}$
12_6	s	91.68 21	45.02 [c]	79.84 16	----------	53.60	4587.58 $\overline{36}$[b]
12_6	a	4201.76 09	55.02 [c]	89.76 34	----------	63.40 [c]	97.31 $\overline{05}$
12_7	s	4199.83 14	53.74 [c]	89.09 33	----------	46.58 $\overline{111}$[b]	80.94 $\overline{108}$
12_7	a	4211.07 67	64.91 [c]	4700.17 57	----------	57.48 07	91.78 $\overline{12}$
12_8	s	08.11 37	62.66 [c]	4698.61 31	----------	39.50 $\overline{94}$	74.33 $\overline{120}$
12_8	a	20.74 120[b]	75.20 113	4711.05 110	----------	51.71 $\overline{16}$	86.45 $\overline{10}$[c]
12_9	s	16.41 [c]	71.69 [c]	08.31 61	----------	32.28 $\overline{38}$	67.62 $\overline{55}$[b]
12_9	a	30.87 85[b]	85.98 87	----------	----------	46.14 $\overline{05}$	81.41 $\overline{03}$[b]
12_{10}	s	24.68 84	80.78 [c]	----------	----------	24.78 $\overline{108}$	60.73 $\overline{89}$[b]
12_{10}	a	41.36	97.31 [c]	----------	----------	40.77 03	76.62 01
12_{11}	s	32.85 50[c]	89.82 43	----------	----------	16.93 [c]	53.65 $\overline{03}$
12_{11}	a	52.43 36[c]	4509.25 17	----------	----------	35.66 10	72.16 02
12_{12}	s	40.94 67	----------	----------	----------	08.58	45.95 36
12_{12}	a	63.97	----------	----------	----------	30.85 01	68.07 $\overline{05}$

See footnotes at end of table.

TABLE 5. *Calculated and observed frequencies in* $\nu_2+\nu_3$, NH_3—Continued

J'_K	p''	^PR	^RR	J'_K	p	^RR
13_0	s	4643.80 22	4642.53 $\overline{29}$	14_1	a	4650.26 $\overline{116}$
13_0	a	50.30 35	----------	14_4	a	35.88 07^b
				14_5	a	29.87 $\overline{26}$
13_1	s	51.48 38	29.24 $\overline{07}^b$	14_6	a	24.12 $\overline{25}$
13_1	a	58.03	35.92 03^b	14_7	a	18.63 $\overline{29}$
				14_8	a	13.36 $\overline{06}^c$
13_2	s	60.60 35	22.31 21^c	14_9	a	08.33 $\overline{16}$
13_2	a	65.04 44	29.26 $\overline{09}^b$			
				14_{10}	s	4591.80 ^{c}
13_3	s	67.44	15.50 32^c	14_{10}	a	4603.53 $\overline{17}$
13_3	a	74.53 67	22.85 $\overline{08}^b$			
				14_{11}	s	4585.26 $\overline{22}$
13_4	s	76.16 38^c	08.84 $\overline{17}^c$	14_{11}	a	99.01 $\overline{06}$
13_4	a	83.58 18^c	16.76 $\overline{14}$			
				14_{12}	s	78.44 $\begin{cases}\overline{154}\\ 142\end{cases}$
13_5	s	84.95 56	02.41 22	14_{12}	a	94.78 $\overline{08}$
13_5	a	92.89 78^b	10.94 $\overline{25}$			
				14_{13}	s	71.11 $\begin{cases}\overline{86}\\ 202\end{cases}$
13_6	s	94.04 61	4596.04 17	14_{13}	a	90.84 $\overline{03}$
13_6	a	4702.69 110	4605.39 $\overline{22}$			
				14_{14}	s	63.16 08^c
13_7	s	03.41 98	4589.61 $\overline{24}$	14_{14}	a	87.34 $\overline{12}$
13_7	a	12.97	4600.10 $\overline{19}^b$			
				15_{13}	a	4603.67 $\overline{18}$
13_8	s	13.01	4583.24 01^c	15_{14}	a	4599.90.01
13_8	a	----------	95.07 $\overline{19}$			
				15_{15}	s	71.34 $\begin{cases}\overline{109}\\ 179\end{cases}$
13_9	s	----------	76.53 $\overline{145}$	15_{15}	a	96.70 $\overline{18}$
13_9	a	----------	90.28 $\overline{07}$			
				16_{16}	s	4579.25 $\begin{cases}\overline{235}\\ 61\end{cases}$
13_{10}	s	----------	69.68 $\begin{cases}\overline{236}^b\\ 57\end{cases}$	16_{16}	a	4605.90 $\overline{29}$
13_{10}	a	----------	85.77 00			
13_{11}	s	----------	62.45 $\begin{cases}\overline{329}\\ \overline{45}\end{cases}$			
13_{11}	a	----------	81.59 23			
13_{12}	s	----------	54.70 $\begin{cases}\overline{270}\\ 170\end{cases}$			
13_{12}	a	----------	77.80 $\overline{09}^b$			
13_{13}	s	----------	----------			
13_{13}	a	----------	----------			

[a] Blend, principally due to calculated line.
[b] Blend, approximately one-half due to calculated line.
[c] Blend, principally due to other line.

should be approximately proportional to the area of the observed absorptions. In figures 1 and 2 this is seen to be the case, with very few exceptions, and it will be further noted that practically all of the observed absorption has been accounted for.

The central panel of figure 1 covers the region of the ^QQ-branches, in which the inversion-doublet separations range from 18 cm^{-1}, for levels with $J \gg K$, to >30 cm^{-1} for $J>12$ in the series with $J=K$, which includes the most intense lines. Throughout this region, and in the other panels of figure 1, there fall the lines of the ^PP- and ^RP-branches. Since the perpendicular bands are more intense by a factor of about seven, the individual lines in them are the strongest single lines in the region, although not as prominent a feature as the parallel Q-branches. In the top panel, the perpendicular lines are becoming weaker; the ^QP-branch "lines" are obvious, and show resolution of the K-structure, the low-K components lying at lower frequencies in the a-s and at higher frequencies in the s-a members of the inversion doublet.

In figure 2 the region covered is that near the origin of the perpendicular bands. ^QR-lines are present but are relatively weak. The J-divergence of the ^RQ-and ^PQ-branches with the same ΔK is considerable, high-J components lying at lower frequencies in both inversion-doublets. The inversion doubling ranges from 21.4 cm^{-1} at ^RQ (11,11) to 8.7 cm^{-1} for ^PQ (11,0).[6] In the bottom panel of figure 2 the ^RR series dominate the absorption.

A further extension to higher frequencies is shown in figure 3. As one proceeds to higher frequencies the intensities drop rapidly in the ^RR-branches, and somewhat less rapidly in the ^PR-branches, so that the latter are the strongest beyond 4,600 cm^{-1}. Even though one is dealing here with very weak lines from levels of high J, it will be noted that a quite complete identification has been achieved. Above 4,680 cm^{-1}, lines of higher-frequency bands begin to appear.

The constants of the NH_3 molecule needed to fit eq (3) and (4) to the line-position data were derived in the following manner. For the ground state, combination differences Δ_1F and Δ_2F were obtained from all pairs of lines listed in tables 4 and 5 that did not involve heavy blends. The combination differences were larger by a few hundredths of a wave number in the s inversion substates than in

[6] For a few observed levels with $K'=2$ the doubling is even lower, because of the (A_1A_2) interaction. Both components of ^PR (12,3) appear, split by only 4.44 cm^{-1}.

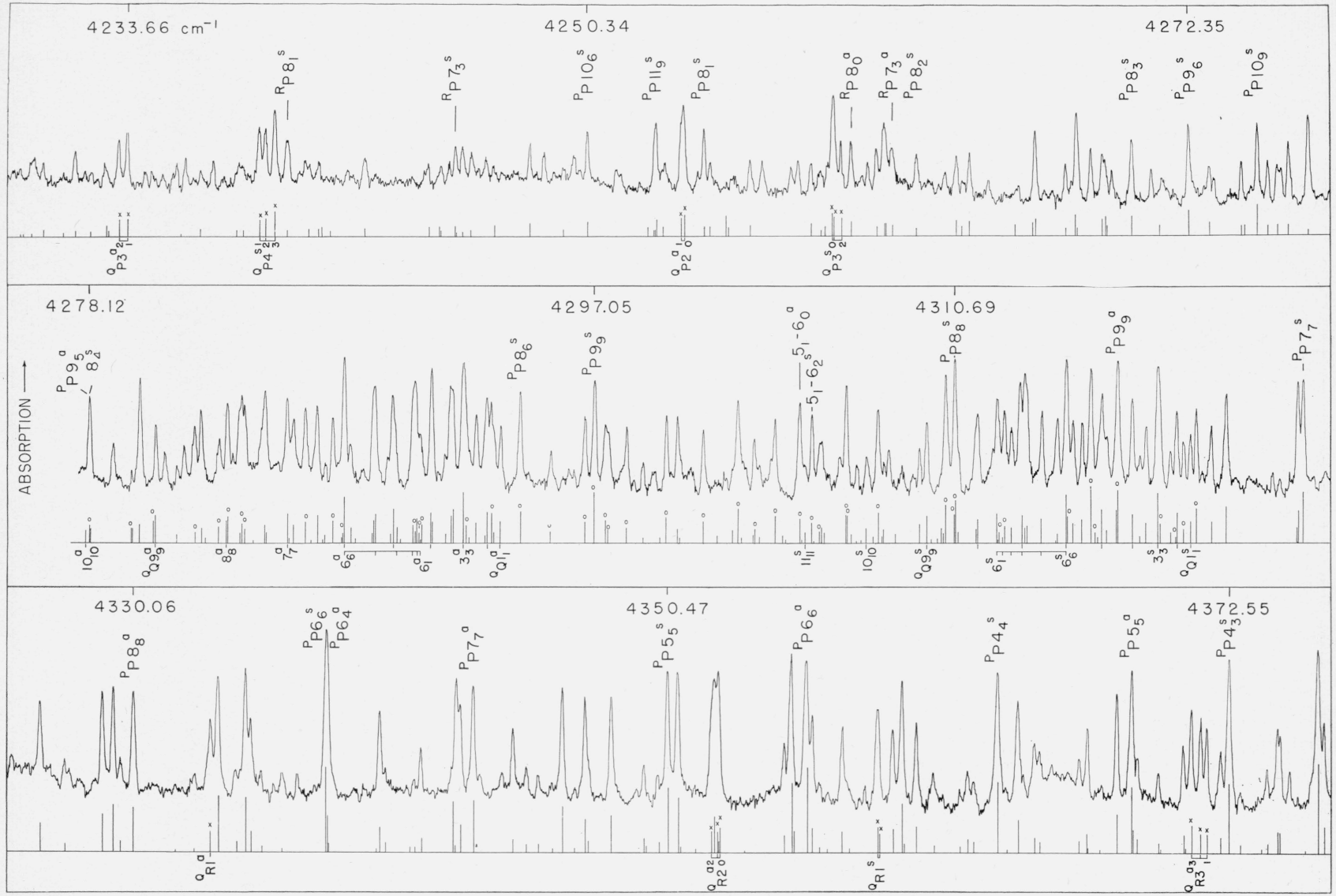

FIGURE 1. NH_3 *spectra, 4,230 to 4,380 cm*$^{-1}$.

Cell length, 10 m; pressure, <1 cm (Hg). Calculated positions and relative intensities are indicated. Lines of the parallel bands $\nu_1+\nu_2$ are distinguished by x in panels 1 and 3; lines of the perpendicular bands $\nu_2+\nu_3$ by 0 in the central panel. Some prominent features are labeled by branch and $(J\,{}^{p}_{K})''$.

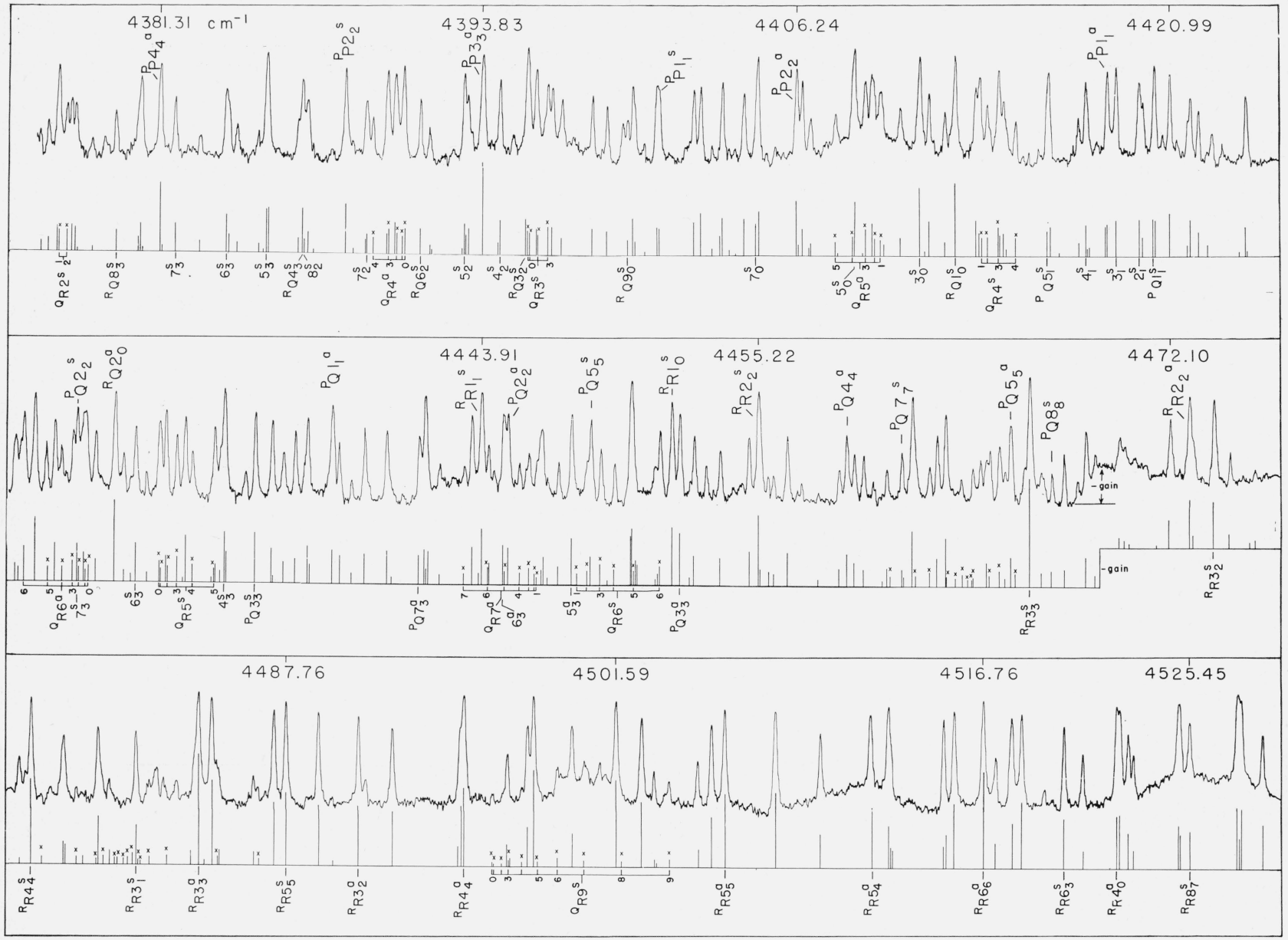

FIGURE 2. NH_3 *spectra, 4,380 to 4,530 cm*$^{-1}$.

Cell length, 10 m; pressure, <1 cm (Hg). Calculated positions and relative intensities are indicated. Lines of the parallel bands $\nu_1+\nu_2$ are distinguished by x. Some prominent features are labeled by branch and $(J^p_K)''$.

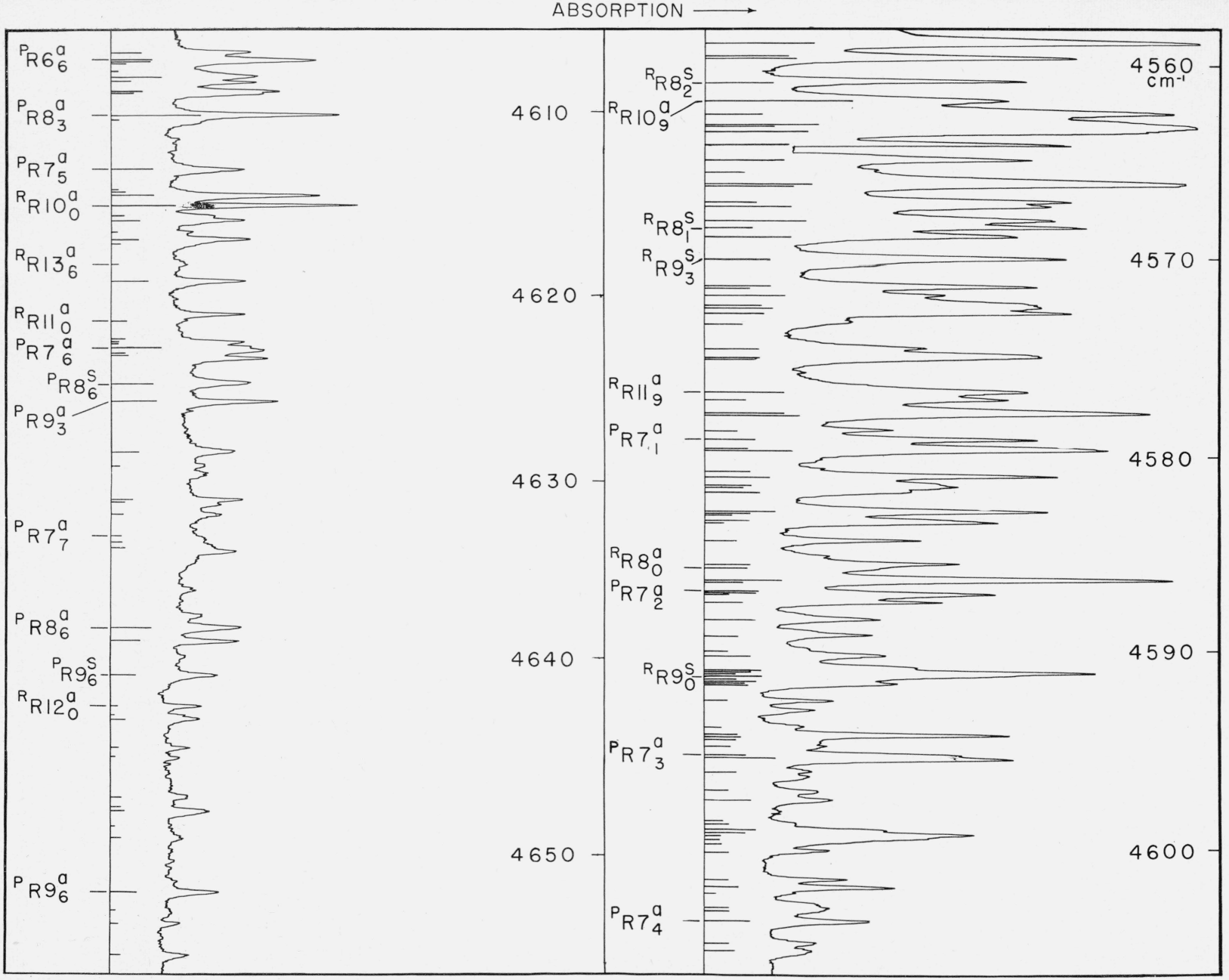

FIGURE 3. NH_3 *spectra, 4,560 to 4,660 cm*$^{-1}$.

Cell length, 10 m; pressure, 9 cm (Hg). Calculated positions and relative intensities are indicated. Some prominent features are labeled by branch and $(J^{P}_{K})''$.

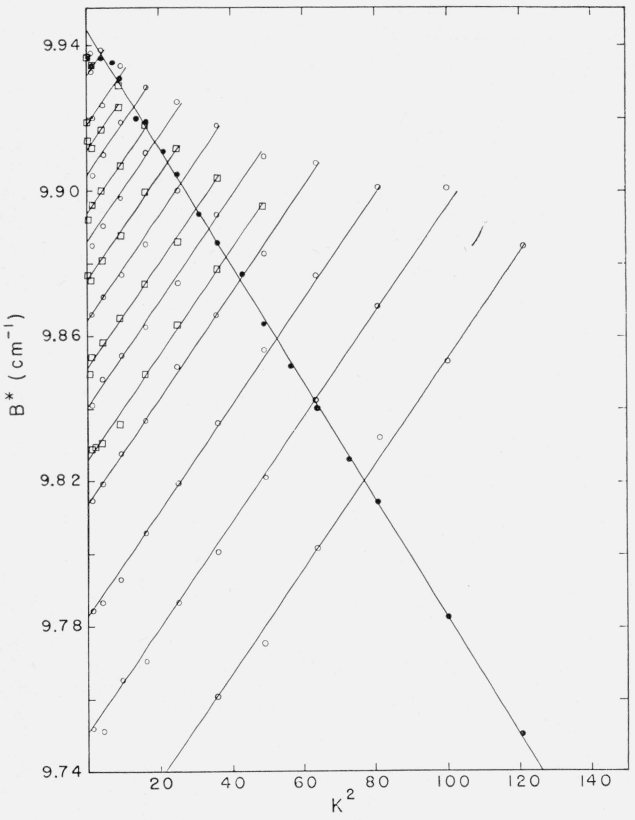

FIGURE 4. *Derivation of rotational constants for* NH_3 *ground state.*

Open circles, $\Delta_2F/(4J+2)$; open squares, $\Delta_1F/2J$. The intercepts of these lines at $K=0$ are plotted as solid circles against $J(J+1)$.

the a substate, as required by eq (4). Inasmuch as infrared measurements cannot be as precise as those in the microwave regions, no attempt was made to determine the ground-state inversion constants, those cited above [17] being accepted. The s and a combination differences were averaged and divided by $2J$ (for Δ_1F) and $(4J+2)$ for Δ_2F. The results are plotted as a function of K^2 as the open points in figure 4; these very nearly form a family of straight lines of equal slope, yielding $D_0^{JK}=-0.001455$ cm^{-1}. The intercepts at $K=0$ are also plotted in figure 4 as solid points as a function of $J(J+1)$; from the slope and intercept of this line is obtained $D_0^J=0.000809$ cm^{-1} and $B_0=9.94428$ cm^{-1}. The combination differences ΔF are given in table 6 as calculated from these constants, and are compared with the observed averages. The agreement is satisfactory. A somewhat better fit might perhaps have been obtained by including sixth-power terms in J and K; that is, by fitting the points in figure 4 to slightly curved parabolas instead of straight lines. It is believed, however, that the precision with which the data are known does not warrant such a procedure at this time; after other bands have been measured with comparable precision, their ground-state combination differences may be included in the averages and improved constants should result.

In order to obtain the constants for the upper states the position of each observed level is first determined relative to the same level in the ground state. For a Q-branch line this is the line position; for P- or R-branch lines, the appropriate ground-state combination differences must be added or subtracted from the observed position. For the parallel bands, there are two observed levels for each (J,K); for the perpendicular bands, four. Straight-line plots of the averages of these, against $J(J+1)$ and K^2, yield ν_0, B_v-B_0, and $[(C_v-C_0)-(B_v-B_0)]$. There appear to be slight but regular deviations from linearity, in the plots against $J(J+1)$, so that it is experimentally justifiable to include the term in $D_v^J-D_0^J$; however, $D_v^{JK}-D_0^{JK}$, and $D_v^K-D_0^K$ appear to be negligible in both bands. The constants are listed in table 7.

The inversion splitting in $\nu_1+\nu_2$ is the difference between the observed Q-branch doublings as obtained above and the ground-state splitting. When plotted against $J(J+1)$ and K^2, considerable curvature is noted. This may be largely eliminated by plotting the logarithm of the splitting; that is, by fitting the rotational dependence to eq (4) instead of to a simple power series. The same behavior is noted in $\nu_3+\nu_2$, for which the inversion splitting is the sum of the ground-state splitting and the observed Q-doublings. Here it is noted that the inversion splitting is slightly different in the K^+ pairs (^RQ-branches) than in the K^- pairs (^PQ-branches). The differences are nearly proportional to K, and hence may be interpreted in terms of a different ζ for the two inversion levels. The average $(K^++K^-)/2$ splitting is used to derive the constants in eq (4). These constants are also given in table 7, as are the constants for each subband of the inversion doublet obtained by converting to the power-series expansion.

The constants C_0, C_v, ζ, and the associated centrifugal-stretching constants are obtained for $\nu_2+\nu_3$ from the differences $(^PQ-{}^RQ)$ as averaged with the corresponding P- and R-lines, and averaged for the two inversion states. From eq (3)

$$[^PQ(J',K')-{}^RQ(J'K')]/4K=(B_0-C_0+C_v\zeta_v+2D_0^K)+(D_0^{JK}-\tfrac{1}{2}\zeta_v^J)J(J+1)+(2D_0^K-\tfrac{1}{2}\zeta_v^K)K^2. \quad (9)$$

The data fit rather well the equation $(^PQ-{}^RQ)/4K=3.9485-0.001206\,J\,(J+1)+0.001462K^2$. Using the already derived values of B_0 and D_0^{JK}, the constants listed in table 7 are obtained. Although there is an experimental value for C_0-C_v, the constants C_0 and ζ, and D_0^K and ζ^K cannot be obtained from this band alone. Only from corresponding measurements in a number of perpendicular bands will it be possible to separate accurately the contributions of the upper and lower states. This will be discussed in a later paper. Tentative values are $C_0=6.196$ cm^{-1}, $D_0^K=7.5\times10^{-4}$ cm^{-1}; whence follow the values of ζ given in table 7. A linear fit to the difference in $^PQ-{}^RQ$ for the a and s components yielded the difference in ζ tabulated.

TABLE 6. *Ground-state combination differences (cm^{-1})*

The first line, for each ΔJ and K in the table, gives the calculated values for the combination difference for the average of the two ground states, s and a, $\pm(s-a)/2$. The second line gives the average values observed in the $(\nu_1,\nu_3+\nu_2)$ bands, the value for the s state being to the left, for the a state to the right, both with the figures preceding the decimal point omitted. When there is no entry on the second line, the corresponding lines have not been observed sufficiently free from blends to yield a reliable value.

ΔJ	K=0 →	1	2	3	4	5	6
2−0	59.636−.014						
	.56						
2−1	----------	39.757±.010					
		.76 .74					
3−1	99.323+.022	99.338±.024					
	.36	.33 .33					
3−2	----------	59.581±.014	59.607±.015				
		.59 .60	.62 .60				
4−2	138.924−.030	138.945±.032	139.005±.034				
	.87	.06 .89	.96 .95				
4−3	----------	79.364±.018	79.398±.019	79.457±.020			
		.38 .33	.39 .36	.48 .44			
5−3	178.390+.038	178.417±.040	178.495±.041	178.626±.045			
	.44	.46 .34	.55 .45	.71 .63			
5−4	----------	99.053±.022	99.097±.022	99.169±.023	99.271±.025		
		.10 .98	.11 .08	.20 .15	.30 .27		
6−4	217.670−.045	217.703±.046	217.800±.047	217.939±.049	218.183±.052		
	.61	.72 .69	.83 .76	.98 .91	.25 .14		
6−5	----------	118.650±.024	118.702±.025	118.790±.026	118.912±.028	119.069±.030	
		.62 .61	.72 .65	.80 .74	.97 .87	.14 .05	
7−5	256.742+.049	256.780±.050	256.895±.052	257.082±.055	257.348±.058	257.688±.062	
	.78	.79 .74	.00 .79	.16 .00	.42 .29	.80 .61	
7−6	----------	138.130±.026	138.191±.027	138.293±.029	138.436±.030	138.619±.032	138.843±.036
		.13 .10	.24 .14	.31 .24	.42 .36	.63 .56	.89 .82
8−6	295.565−.051	295.607±.052	295.739±.054	295.937±.054	296.262±.061	296.656±.065	297.135±.073
	.48	.68 .51	.85 .68	.99 .89	.25 .20	.64 .51	.20 .01
8−7	----------	157.478±.026	157.548±.027	157.664±.024	157.827±.031	158.037±.033	158.293±.037
		.53 .36	.57 .55	.68 .66	.81 .78	.01 .98	.31 .27
9−7	334.093+.052	334.142±.053	334.292±.055	334.548±.065	334.884±.062	335.330±.068	335.874±.074
	.16	.17 .16	.26 .21	.58 .48	.92 .86	.40 .30	.92 .80
9−8	----------	176.664±.026	176.743±.028	176.874±.040	177.057±.031	177.293±.034	177.581±.037
		.69 .64	.73 .73	.96 .77	.09 .00	.33 .27	.60 .55
10−9	----------	195.679±.026	195.766±.027	195.912±.008	196.115±.030	196.377±.033	196.697±.037
		.69 .64	.74 .74	.94 .79	.17 .06	.46 .33	.77 .65
11−10	----------	214.499±.025	214.595±.026	214.755±.066	214.979±.029	215.267±.031	215.619±.035
		.57	.50	.85 .83	.98	.39 .24	.61 .62
12−11	----------	233.106±.024	233.211±.024	233.385±.038	233.630±.027	233.944±.030	234.328±.032
			.48	.41			.39 .11
13−12	----------	251.480±.022	251.593±.023	251.782±.128	252 047±.025	252 388±.027	252.804±.030
14−13	----------	269.601±.020	269.723±.021	269.927±.143	270.212±.023	270.579±.025	271.027±.028

ΔJ	K=7 →	8	9	10	11	12	13
8−7	158.596±.041						
	.63 .51						
9−7	336.518±.083						
	.41						
9−8	177.921±.042	178.314±.048					
	.94 .87	.38 .28					
10−9	197.074±.041	197.512±.047	198.007±.055				
	.13 .11	.59 .48	.05 .97				
11−10	216.036±.039	216.516±.045	217.060±.052	217.668±.062			
	.21 .91	.56 .47	.11 .08	.87 .77			
12−11	234.782±.036	235.306±.042	235.899±.049	236.563±.058	237.296±.070		
	.57	.17 .29	.14 .83	.42	.16		
13−12	253.296±.034	253.863±.038	254.506±.045	255.225±.054	256.019±.064	256.889±.080	
						.99	
14−13	271.557±.031	272.168±.035	272.860±.040	273.634±.048	274.490±.058	275.427±.072	276.445±.090

The upper-state levels with $K=1^+$ and 2^- (A_1, A_2 doublets) deviated from the positions calculated with the over-all constants in approximately the way required by eq (4b) and (4c). The resulting constants were $\beta_{1,0110}=1.95\times10^{-2}$ cm^{-1}; $\beta_{2,0110}=1.88\times10^{-4}$ cm^{-1}.

The constants summarized in table 7 give, as tables 4 and 5 show, an excellent representation of the observed spectra up to $J=10$. There are increasing deviations of the observed from calculated lines at higher J. These arise partly from the difficulties of measuring the weak lines of high J', partly from the failure to include additional terms of higher order in the energy expressions, and presumably, to some extent from additional perturbations on the upper-state energy not included in the standard expressions. It will be noted that when the (obs-calc) deviations in the tables are greater than 0.1 cm^{-1}, the deviations for the three lines with a common upper state agree, behavior which is typical of an upper-state perturbation. A partial quantitative explanation can be given for two of these perturbations, which will now be discussed briefly.

TABLE 7. *Molecular constants for* NH_3 *bands* ($\nu_1+\nu_2$ *and* $\nu_2+\nu_3$)

Constants	Units	Band: $\nu_1+\nu_2$			Band: $\nu_3+\nu_2$			Ground-state value
		$s-a$	$a-s$	Average	$a-s$	$s-a$	Average	
ν_0	cm^{-1}	4293.716	4320.060	4306.888	4416.908	4434.610	4425.759	----------
B_v-B_0	$10^{-2}cm^{-1}$	−6.22	−19.38	−12.80	−15.087	−24.421	−19.754	994.43
$(C-B)_v-(C-B)_0$	$10^{-2}cm^{-1}$	−9.83	8.23	−0.80	4.414	17.839	11.126	(−376.9)
C_v-C_0	$10^{-2}cm^{-1}$	−16.05	−11.15	−13.60	−10.673	−6.582	−8.628	(617.5)
$D_v^J-D_0^J$	$10^{-4}cm^{-1}$	1.25	−2.05	−0.4	0.70	−1.90	−0.60	8.09
$D_V^{JK}-D_0^{JK}$	$10^{-4}cm^{-1}$	−4.5	4.5	0	−3.91	3.14	−.38	−14.55
$D_v^K-D_0^K$	$10^{-4}cm^{-1}$	3.1	−3.1	0	3.52	−1.56	.98	(7.5)
$C_0-2D_0^K-C_v\zeta$	cm^{-1}	----------	----------	----------	6.0065	5.9850	5.9958	----------
ζ	----------	----------	----------	----------	0.0273	0.0310	0.0292	----------
ζ^J	$10^{-4}cm^{-1}$	----------	----------	----------	----------	----------	−4.98	----------
$D_0^K-\frac{1}{4}\zeta^K$	$10^{-4}cm^{-1}$	----------	----------	----------	----------	----------	7.31	----------
E_v^i	cm^{-1}	----------	----------	25.551	----------	----------	18.495	0.7934
b_v^i	10^{-3}	----------	----------	−4.95	----------	----------	−5.32	−6.3700
$C_v^i-b_v^i$	10^{-3}	----------	----------	6.79	----------	----------	7.64	8.8899
C_v^i	10^{-3}	----------	----------	1.84	----------	----------	2.32	2.5199
d_v^{iJ}	10^{-6}	----------	----------	0?	----------	----------	0.83	0.8692

The three levels v_1, J, K; v_3, J, $(K+1)^+$; and v_3, J, $(K-1)^-$ are of identical over-all symmetry, and interact due to Coriolis forces. The matrix of the interaction is

	$K-1$	K	$K+1$
$K-1$	$\nu_3+E_r(J,K-1)-E$	$\frac{\alpha}{\sqrt{2}}[(J+K)(J-K+1)]^{1/2}$	0
K	$\frac{\alpha}{\sqrt{2}}[(J+K)(J-K+1)]^{1/2}$	$\nu_1+E_r(J,K)-E$	$\frac{\alpha}{\sqrt{2}}[(J-K)(J+K+1)]^{1/2}$
$K+1$	0	$\frac{\alpha}{\sqrt{2}}[(J-K)(J+K+1)]^{1/2}$	$\nu_3+E_r(J,K+1)-E$,

(10)

where $\alpha=\frac{1}{2}\zeta_{13}B_e(\omega_1+\omega_3)/(\omega_1\omega_3)^{1/2}$, and ζ_{13} is the interaction constant. When, as is the case for most values of K, the energy difference between the interacting levels is large compared with the off-diagonal matrix elements, the latter terms make the normal second-order contributions to the energy that appears as part of the constants $\alpha_1{}^B$ and $\alpha_3{}^B$. When, however, the energy difference becomes of the same order of magnitude as $\alpha[(J-K)(J+K+1)]^{1/2}$ a perturbation occurs, attaining its maximum effect when the two states coincide. The energy differences, neglecting the perturbations and centrifugal-stretching terms, are

$$E_{JK\pm1}-E_{JK}=\nu_3-\nu_1\pm(2K+1)[C_3(1\pm\zeta)] -C_1-B_3+B_1, \quad (11)$$

i. e., it approaches zero for the state $K+1$, corresponding to approach of the lines in the ${}^QQ$- and ${}^RQ$-branches at high K. In the a-s half-band of $\nu_2+\nu_3$, the constants are such that $\Delta E\sim0$ at $K\sim13$; in the s-a half-band, $\Delta\nu_0$ is greater, so that the cross-over is at slightly higher K. As is apparent from table 5, the series of strong ${}^RR$ lines with $K=J$ can be followed in s-a to $K'=15$, whereas in a-s the sequence becomes irregular. No line of the expected intensity can be found near the calculated positions for ${}^RR(13,13)$, but two lines of nearly equal strength otherwise unaccounted for occur at frequencies 2.70 cm^{-1} below and 1.70 cm^{-1} above the calculated value of 4554.70 cm^{-1}. It is tempting to assign these to the perturbed level. If the resonance is exact, the derived value of $\alpha=4.40/26=0.17$, corresponding to

$\zeta_{13}=0.017$. This is of the theoretically expected order of magnitude. α is so small that the levels with $K^+<12$, for which $\Delta E>16$ cm^{-1}, would not be shifted greatly from their unperturbed positions, so that the normal method of deriving molecular constants is justifiable, the bulk of the effect of the perturbation being taken up in $D_v^J-D_0^J$. The perturbation would, however, account for the deviations (obs-calc) of from 0.1 to 1 cm^{-1} found in the (a-s) band for $J\gtrsim 11$, which can be fitted only by powers of $(J+K)$ higher than the fourth.

The second perturbation would arise from the resonances caused by the near equality of $2\times\nu_4$ and ν_1. In the present instance the levels $2\nu_4^0+\nu_2$ lie about 100 cm^{-1} below $\nu_1+\nu_2$ for each J_K, and are of like symmetry. Each level of $\nu_1+\nu_2$ will thus be pushed upward; the shifts would be equal if the rotational constants and inversion doubling were the same in $2\nu_4^0+\nu_2$ and $\nu_1+\nu_2$. However, because the observation of other bands involving ν_4 indicates that the inversion doubling will be considerably greater in $2\nu_4+\nu_2$ than in $\nu_1+\nu_2$, and that $B_4>B_2$, the resulting perturbations on the $\nu_1+\nu_2$ levels, particularly those of high J in the upper (a) inversion state, may become too large to fit by the normal power series. Table 4 shows that the deviations are indeed greatest for those levels. The $2\nu_4^2+\nu_2$ levels, as well as those of $2\nu_4^0+\nu_2$ will also interact Coriolis-wise with those of $\nu_3+\nu_2$, however, these effects are presumably of less importance than those discussed in the previous paragraph because the energy differences are greater.

Although, as just mentioned, the states of $2\nu_4+\nu_2$ lie close enough to $\nu_1+\nu_2$ to affect the latter, and their position can be estimated with some probability, it has not as yet been possible to identify any of the lines in those bands. There are a number of quite strong lines below 4,200 cm^{-1} that must belong to the bands, and these are particularly numerous near 4,180 and 4,130 cm^{-1}, where the ^qQ-branches should lie, but no convincing assignment of the strong lines to the expected series has been achieved. Presumably the many possible interactions disturb the intensities, as well as the positions of the expected transitions. In the corresponding bands of ND_3, however, a satisfactory analysis has been achieved, with normal intensities, so that the difficulties encountered in NH_3 remain puzzling.

3.2. Line and Band Strength and Line Width

The problems of relating the observed fractional transmission of a resolved spectrum to the true strength and shape of its component lines have been discussed in detail elsewhere [7]. There are two principal types of difficulties, aside from the experimental problems of accurate measurement of absorbing conditions and transmission. The first arise when the spectrometer slit width is appreciably greater than the line width; these can be overcome if it is possible to obtain measurements at a variety of pressures and path lengths on single lines, free from overlapping by neighboring lines in the spectrum. The second type of difficulties arise from overlapping, and are imposed by the nature of the spectrum. In NH_3 vibration-rotation bands in general, the self-broadened line widths are quite high, from 0.15 to 0.6 cm^{-1}/atm. This is a consequence of the high dipole moment (1.46 Debyes) and the low inversion frequency of the ground state. As a result, with the effective resolution of $\sim$0.10 cm^{-1} available in the region 1,600 to 7,500 cm^{-1}, slit corrections should become of minor significance at pressures of ⅓ atm and above. Unfortunately, however, in nearly all NH_3 bands the lines are closely spaced, so that overlapping becomes a major problem.

In the bands reported in the present paper, there are only a few regions where overlapping at $P>⅓$ atm is not serious, so that the absolute widths of only those few lines may be determined with fair accuracy. However, from low-pressure measurements the relative strength-width products of most of the lines can be determined, and from high-pressure measurements the strengths may be found. These results are given in this section. Much more satisfactory measurements of the strength, width, and shape of NH_3 vibration-rotation lines have been achieved in the parallel bands $3\nu_2$, where $(B_0-B_v-C_0+C_v)$ is sufficiently large so that overlap is at a minimum. These will be presented in a subsequent paper.

The band strengths, S_v of the perpendicular and parallel bands were determined by two methods. First, by measurement of the integrated absorption in those portions of the bands where such measurements are meaningful, making corrections for overlap of the bands. Second, by measurement of the equivalent width and hence the strengths of individual lines that fell in the near-linear region of the curve of growth, assuming that the band strength is related to the line strength by eq (5).

The first method requires measurements at pressures greater than 30 cm, so that the slit corrections may be neglected, and path lengths such that the absorption is in the range 10 to 90 percent, where the measurements are least subject to experimental error resulting from uncertainties in locating the base lines. These conditions are met in the 5-cm cell for the central region of the bands, from 4,280 to 4,560 cm^{-1}, covering the Q- and R-branches of the weaker bands $\nu_1+\nu_2$, and the main portion of the stronger band $\nu_3+\nu_2$. The 15.5-cm cell provides checks on the regions of weaker absorption in that interval, and in addition provides data on the regions 4,160 to 4,280 cm^{-1}, where lines of the P-branch of $\nu_1+\nu_2$ are relatively free from overlap by other bands, and 4,560 to 4,600 cm^{-1}. The results obtained are for $\nu_1+\nu_2$, $S_v^0=2.9\pm0.5$ cm^{-2} atm^{-1}, and for $\nu_3+\nu_2$, $S_v^0=19.7\pm2$ cm^{-2} atm^{-1}. The above figures refer to an average temperature of 296°K (although the integrated band strength appears, as expected, not to be significantly temperature-dependent), and the pressure refers to the actual temperature, not 273°K.

The best possibilities for measuring strengths of individual lines in $\nu_2+\nu_3$ are in the extreme wings ($J>9$, ^PR- and ^RP-branches), and for those few lines at low J in ^RR and ^PP where the nearest neighbors are more than 1 cm^{-1} distant. The 1,000-cm path provided numerous examples of the first type, the 15.5-cm path several of the second. For these the mean specific

equivalent widths, W/P, are collected and averaged in table 8. The corrections to the observed W/P for the effect of line width were made according to the formula [7]

$$S_{vr}^{0}l=(W/P)(1+W/2\pi\gamma^{0}P), \tag{11}$$

which is valid when $W/2\pi\gamma^{0}P<0.5$. The correction involves the linewidth γ^{0}, for which the smoothed values to be described later were used, but the average results are not significantly dependent on the choice of γ^{0}. It will be noted that the observed equivalent widths for the two components of the inversion doublet are in rough agreement, so that their average value was used in the subsequent computations. For each line, using the rigid-rotator value of $S_{v}r/S_{v}$ (table 3), a value of S_{v}^{0} (rig) was calculated. If the measurements were precise, and the assumption F=1 valid, these should all be equal to 19.7 cm^{-2} atm^{-1} as obtained from the integrated-band measurements. Considerable variation will be noted, although the agreement is always within a factor of two. The presence of unsuspected blends may occasionally give rise to abnormally high values of S_{v}^{0}; these were excluded from the averages. The group averages show regularities, in that the ${}^{P}R$ lines are significantly weaker, and the ${}^{R}P$ lines significantly stronger, than the average, while ${}^{R}R$ and ${}^{P}P$ show similar but less-marked deviations. It thus appears likely that the observations reveal effects of the vibration-rotation interaction on the intensities. The approximate form of the interaction factor F for a perpendicular band of a symmetric-top is [19]

$$F=(1+am+bk)^{2}$$

where m is the ordinal line number in a K sub-branch (J' in ${}^{R}R$ and ${}^{P}R$, $-J''$ in ${}^{R}P$ and ${}^{P}P$), and k the ordinal number of the sub-branch (K' in ${}^{R}P$, ${}^{R}Q$, and ${}^{R}R$; $-K''$ in ${}^{P}P$, ${}^{P}Q$, and ${}^{P}R$). a and b are constants that in principle might be evaluated from the absolute intensities of all of the vibration-rotation bands and the potential function. Because such full information is lacking, it is sufficient to note that a considerable reduction in the scatter of the results for the $\nu_{2}+\nu_{3}$ band is achieved by using as tentative empirical values, $a=-0.015$, $b=0.01$. The last two columns of table 8 give the resulting values of $F(0110,JK)$ and S_{v}^{0} (corr)$=S_{v}^{0}$ (rig)$/F$. The final value of S_{v}^{0} by this method is 24.0 ± 3 cm^{-2} atm^{-1}. This result is 20 percent higher than obtained by direct integration. The first method is probably slightly the more reliable, its greater uncertainty in locating the zero-absorption level being overcome by the fewer theoretical assumptions involved.

It is interesting to note that the measurements show the $\nu_{2}+\nu_{3}$ combination band to be more intense than the ν_{3} fundamental, for which McKean and Schatz [20] report a value of 13 cm^{-2} atm^{-1} from measurements of the combined absorption in ν_{1} and ν_{3}. From the high-resolution measurements of those fundamentals, to be reported in a subsequent paper, it appears that the relative contribution of ν_{3} to the $\nu_{1}+\nu_{3}$ sum has been underestimated, but in any event the combination band is the more intense. This must reflect the highly anharmonic nature of the ν_{2} vibration, as well as a considerable breakdown of the separation of modes in the combination band.

Having thus established fairly accurate values of the strength of each individual line, there are now three possible methods for obtaining line widths, assuming the Lorentz shape. The first applies at high pressures, (i. e., above 1/3 atm) when the line width 2γ is greater than the slit width d. It is based on the measurement of the extinction at a line peak, where for a single line,

$$\epsilon_{max}=-\ln(I_{min}/I_{0})=(1/\pi l)(S^{0}/\gamma^{0}). \tag{13}$$

The measurement is subject to slit corrections which are functions of γ/d and of ϵ_{max}, which may conveniently be evaluated from the graphs of Kostkowski and Bass [21]. ϵ_{max} should be independent of pressure, except insofar as $\gamma=\gamma^{0}P$ enters into the slit correction. However, as mentioned previously, at pressures sufficiently high for the slit corrections to be small, the overlap by neighboring lines is appreciable. However, their contribution may be estimated, so that from the observed ϵ and the calculated $S^{0}\gamma^{0}$ is obtained. Reasonably concordant results were obtained for a few isolated lines in the 5- and 15-cm cells.

The second method is applicable to the same lines, where slit-correction effects and overlap effects are both small, and consists of the direct measurement of the line breadth b_{ϵ} at various values of the extinction ϵ. For a Lorentz line,

$$\gamma^{0}P=(b_{\epsilon}/2)[\epsilon_{max}/\epsilon)-1]^{-1/2}. \tag{14}$$

A single measurement of b at $\epsilon=\epsilon_{max}/2$ might suffice to give 2γ directly if observing conditions are very stable. In practice, it is preferable to measure b at several values of ϵ, apply the slit and overlap-corrections, and average the results.

The third method is more generally applicable in these NH_{3} bands, being the measurement of equivalent width under the conditions of long path and low pressure, for which overlapping is minimal. The appropriate relation valid for $x>1$, is

$$W/P=2(S^{0}\gamma^{0})^{1/2}\left(1-\frac{1}{8x}\right), \tag{15}$$

where x is $S^{0}/2\pi\gamma^{0}$. With $l=1{,}000$ cm, x for the strongest line is of the order of 100, so that most of the observed lines should obey the "square-root law" quite closely. Thus $\gamma^{0}=4(W/P)^{2}/S^{0}$. The principal corrections required here, for the suitable spectra obtained over the pressure range 0.5 to 3 cm, arise from the Doppler effect. The parameter governing those corrections is $a=(\ln 2)^{1/2}\,\gamma_{L}/\gamma_{D}$, γ_{L}, and γ_{D} being, respectively, the Lorentz and Doppler widths. For NH_{3} at 298° K and 4,500 cm^{-1}, $\gamma_{D}=0.00674$ cm^{-1}, so that if $\gamma^{0}\cong 0.5$ cm^{-1} atm^{-1}, $a<1$ for $P<0.82$ cm Hg. For $x>5$ the corrections are still very small at the lowest pressures studied, the difficulty of measuring pressures below 1 cm with sufficient accuracy being a greater source of uncertainty.

TABLE 8. *Band strength $\nu_2+\nu_3$ from near-linear lines*

Line	ν	W/P	$S_\nu^0/S_r l$	$\frac{S_r}{10^4 S_\nu}$	S_ν^0 (rig)	F	S_ν^0 (corr)
Weak R-branch lines, l=1,000 cm							
	cm^{-1}	cm^{-1}/cm Hg	cm^{-1}/cm Hg		$cm^{-2}atm^{-1}$		$cm^{-2}atm^{-1}$
$^PR(11, 9)$	4,712	0.0020	0.0025	0.131	13.6	0.53	25.6
	4,699	.0029					
$^PR(10, 9)$	4,698	.0027	.0037	.203	13.1	.56	24.5
	4,684	.0045					
$^PR(11, 7)$	4,690	.0032	.0035	.093	26.6	.56	47?
	4,680	.0035					
$^PR(10, 8)$	4,687	.0025	.0031	.158	14.1	.57	25
	4,674	.0034					
$^PR(9, 9)$	4,684	.0045	.0046	.194	16.9	.58	29
	4,668	.0044					
$^PR(10, 6)$	4,667	.0078	.0079	.460	12.3	.60	20.5
	4,656	.0066					
$^PR(9, 7)$	4,662	.0057	.0063	.329	13.8	.61	23
	4,650	.0061					
$^PR(10, 5)$	4,657	.0035	.0039	.265	10.6	.62	17.3
	4,647	.0038					
$^PR(11, 3)$	4,654	.0035	.0047	.281	12.0	.62	19.2
	4,645	.0053					
$^PR(10, 3)$	4,639	.015	.0167	.693	17.4	.65	27
	4,631	.012					
$^PR(8, 6)$	4,638	.023	.034	1.373	19.3	.65	30
	4,625	.026					
$^RR(11, 3)$	4,600	.014	.0175	0.749	17.0	.74	23
$^RR(11, 4)$	4,603	.0090	0.0107	0.478	15.3	.75	20.3
	4,594	.010					
Average, 23 lines					14.5	---	23.8
Strong R-branch Lines, l=15.5 cm							
$^RR(8, 2)$	4,573	0.00192	0.00198	4.31	22.0	0.78	28
$^RR(6, 3)$	4,566	.0060	.0065	18.74	16.3	.78	21
$^RR(10, 6)$	4,565	.00157	.00160	4.69	16.2	.75	21.5
$^RR(9, 3)$	4,563	.00252	.0026	4.96	25.0	.78	32.5
$^PR(6, 2)$	4,558	.0139	.0145	24.6	28.0	.85	33
$^RR(5, 2)$	4,557	.0099	.0113	26.1	20.5	.87	23.7
$^RR(9, 8)$	4,553	.0045	.0047	12.4	18.3	.87	21.1
$^RR(8, 6)$	4,548	.025	.029	73.5	18.7	.86	21.7
Average, 8 lines					20.6	---	24.0
Strong P-branch lines, l=15.5 cm							
$^PP(4, 2)$	4,347	0.0124	0.0147	28.3	25.8	1.08	23.9
$^PP(6, 5)$	4,346	.0128	.0145	32.6	22.1	1.08	20.4
$^RP(3, 1)$	4,345	.0034	.0036	3.25	59	1.13	52?
$^PP(4, 1)$	4,339	.0076	.0086	17.0	25.3	1.10	23.0
$^PP(8, 8)$	4,330	.0096	.0105	26.8	19.6	1.08	18.2
Average, 4 lines					23.2	---	21.4
Weak P-branch lines, l=1,000 cm							
$^PP(11, 7)$	4,249	0.035	0.068	1.04	51.7	1.19	43.5
	4,236	.040					
$^PP(10, 1)$	4,211	.012	.0157	0.507	24.6	1.30	18.9
$^RP(8, 5)$	4,209	.010	.011	.318	27.4	1.12	24.5
$^RP(10, 1)$	4,207	.010	.0115	.333	27.5	1.34	20.5
$^PP(11, 2)$	4,207	.010	.0115	.244	37.5	1.31	28.6
Average, 5 lines					33.7	---	27.2
Over-all average, 40 lines					19.0	---	24.0

Table 9 summarizes some of the numerous measurements made on four of the best lines by the three methods just outlined. They are in fairly good agreement, indicating that the estimates of S^0, and the various assumptions and measurements are reasonably well founded. Since in the three methods γ^0 is proportional respectively to $(S^0)^{+1}$, $(S^0)^0$, and $(S^0)^{-1}$ uncertainties in S^0 should not affect the average values.

It will be noted that there is a considerable variation in the magnitude of γ^0 for the four lines included in table 9. It is largest for the two lines with $K=J$, and decreases with K/J. The same behavior was noted for the many other lines of the

TABLE 9. *Line-width measurements for selected lines*

Conditions	Line	$^{R}R(3,3)^{s}$	$^{R}R(3,0)^{s}$	$^{R}R(5,2)^{s}$	$^{R}R(6,6)^{a}$
	ν_0 (cm^{-1})	4466.3	4489.1	4510.1	4516.8
	S^0 calc (cm^{-2} atm^{-1})	0.301	0.177	0.0479	0.210
Method 1: l=15.5 cm, P=0.32 atm.	ϵ_{max} (obs.)	2.47	2.95	0.79	2.00
	Slit corr.	+0.10	+0.41	+.09	+0.10
	Overlap corr.	−.06	−.16	−.08	−.13
	ϵ_{max} (corr.)	2.51	3.20	.80	1.97
	γ^0 (cm^{-1} atm^{-1})	0.59	0.27	.29	0.53
Method 1: l=5.0 cm, P=0.91 atm.	ϵ_{max} (obs.)	1.10	1.57	0.40	1.04
	Slit corr.	+0.02	+0.05	+.01	+.02
	Overlap corr.	−.18	−.45	−.22	−.38
	ϵ_{max} (corr.)	.94	1.17	.19	.68
	γ^0 (cm^{-1} atm^{-1})	.51	0.24	.40	.49
Method 2: l=15.5 cm, P=0.32 atm.	Range of $b\epsilon$ (cm^{-1})	0.3 to 0.8	0.15 to 0.5	0.4 to 1.2	0.2 to 0.8
	Corrections, %	12 to 5	18 to 5	18 to 8	20 to 5
	Average γ^0 (cm^{-1} atm^{-1})	0.49±.05	0.22±.04	0.43±.03	0.59±.05
Method 3: l=1,000 cm, P=0.0065 atm.	W obs (cm^{-1})	0.171	0.081	0.056	0.137
	Doppler corr. %	−.5	−2.0	−5.8	−.7
	γ^0 (cm^{-1} atm^{-1})	.57	0.21	0.35	.54
Average observed γ^0 (cm^{-1} atm^{-1})		0.54±.04	0.23±.03	0.37±.05	0.55±.04
Microwave γ^0 (cm^{-1} atm^{-1})		.69	.25	.41	.73

TABLE 10. *Smoothed values of line width γ^0 (cm^{-1} atm^{-1}) in $\nu_2+\nu_3$*

$(J'+J'')/2$												$(K'K'')/2$
½	1½	2½	3½	4½	5½	6½	7½	8½	9½	10½	11½	
0.37	0.31	0.27	0.25	0.24	0.23	0.21	0.19	0.18	0.18	0.17	0.16	½
	.47	.38	.32	.29	.28	.27	.26	.24	.22	.21	.20	1½
		.53	.44	.38	.35	.34	.31	.29	.27	.26	.24	2½
			.55	.47	.42	.40	.37	.34	.30	.28	.26	3½
				.56	.50	.46	.41	.38	.35	.32	.30	4½
					.56	.51	.46	.42	.40	.37	.33	5½
						.57	.51	.47	.44	.42	.39	6½
							.57	.52	.48	.45	.43	7½
								.56	.52	.48	.45	8½
									.55	.51	.47	9½
										.55	.50	10½
											.54	11½

band for which measurements, chiefly by the third method, could be made. The absolute results for any single determination appear rather inaccurate, but the relative values as functions of J and K are quite regular. Smoothed average values are given in table 10. The dependence on J and K parallels that found in the microwave region [6]. Anderson [8] has shown that the observed microwave widths are in good agreement with his theory of collision-broadening. Table 9 includes Anderson's values, averaged for the two states involved. It is apparent that the vibration-rotation widths are consistently 20 to 25 percent less than the microwave widths. An application of Anderson's theory to the present situation has not been attempted, because of the complexity of the calculation and the limited accuracy of the data, but it is qualitatively apparent that a decreased width of the observed order is to be expected. For the microwave case, when the vibrational transition is 0^a-0^s, both initial and final states have inversion frequencies <1 cm^{-1}, so that in all encounters with colliding molecules, nearly resonant dipolar transitions can occur. For the infrared bands $01^{a,s}10-0^{s,a}$, the initial state has the same low inversion frequency, <1 cm^{-1}, but for the upper state the inversion frequency is ~ 20 cm^{-1}. Hence a large proportion of the energy interchanges involving simultaneous dipolar transitions of the upper state and a colliding molecule are farther from resonance, resulting, according to Anderson's theory, in a decreased width. Note also that transitions involving $K=0$, which cannot occur in the microwave Q-branch lines, are the narrowest observed, again as a result of the paucity of resonant interactions involving those states.

According to this qualitative interpretation of the observed width data, in other vibration-rotation bands of NH_3 the widths should be greatest when both states have low resonant frequencies (e. g., ν_3), and should be even narrower than observed here when the upper state has very high inversion frequencies (e. g., $3\nu_2$). Work in progress shows that this is indeed the case.

It is of interest to note that the marked variation in half-width among the lines of the band results in easily recognizable alterations in the general appearance of the absorption under varying conditions. At high pressures and short paths the lines of greatest half-width are least prominent, since $\epsilon_{max} \sim S^0/\gamma^0 P$, whereas at low pressures and long paths they are the most prominent, since $I_{max} \sim W \sim (S^0\gamma^0)^{1/2}$. This is illustrated by the three tracings in figure 5, where the same spectral region is reproduced with identical slit widths for the three conditions 1=1000

cm, P=0.5 cm; 1=15.5 cm, P=24 cm; and 1=5 cm, P=73 cm. In the upper panel, the calculated positions are represented by lines whose height is proportional to $(S^0\gamma^0)^{1/2}$; in the center by lines of height proportional to S^0; (since here γ is of the same order as d) and at the bottom, when overlapping is least extreme, by triangles of width $\sim\gamma^0$ and height $\sim S^0/\gamma^0$. The representations of the spectra are good, and the variations are notable. For example, the line ${}^{R}R(9,8)^{a}$ at 4552.8 cm^{-1} (γ^0=0.52 cm^{-1} atm^{-1}) is barely visible at high pressure, but is prominent at low pressure. Conversely, lines ${}^{R}R(6,0)^{a}$ and ${}^{R}R(7,0)^{s}$, with γ^0=0.20 cm^{-1} atm^{-1}, are very prominent at high pressure, and relatively weak at low pressure.

As a consequence of this variation, it may be pointed out that sets of spectra such as those in figure 5 may be used to distinguish narrow from

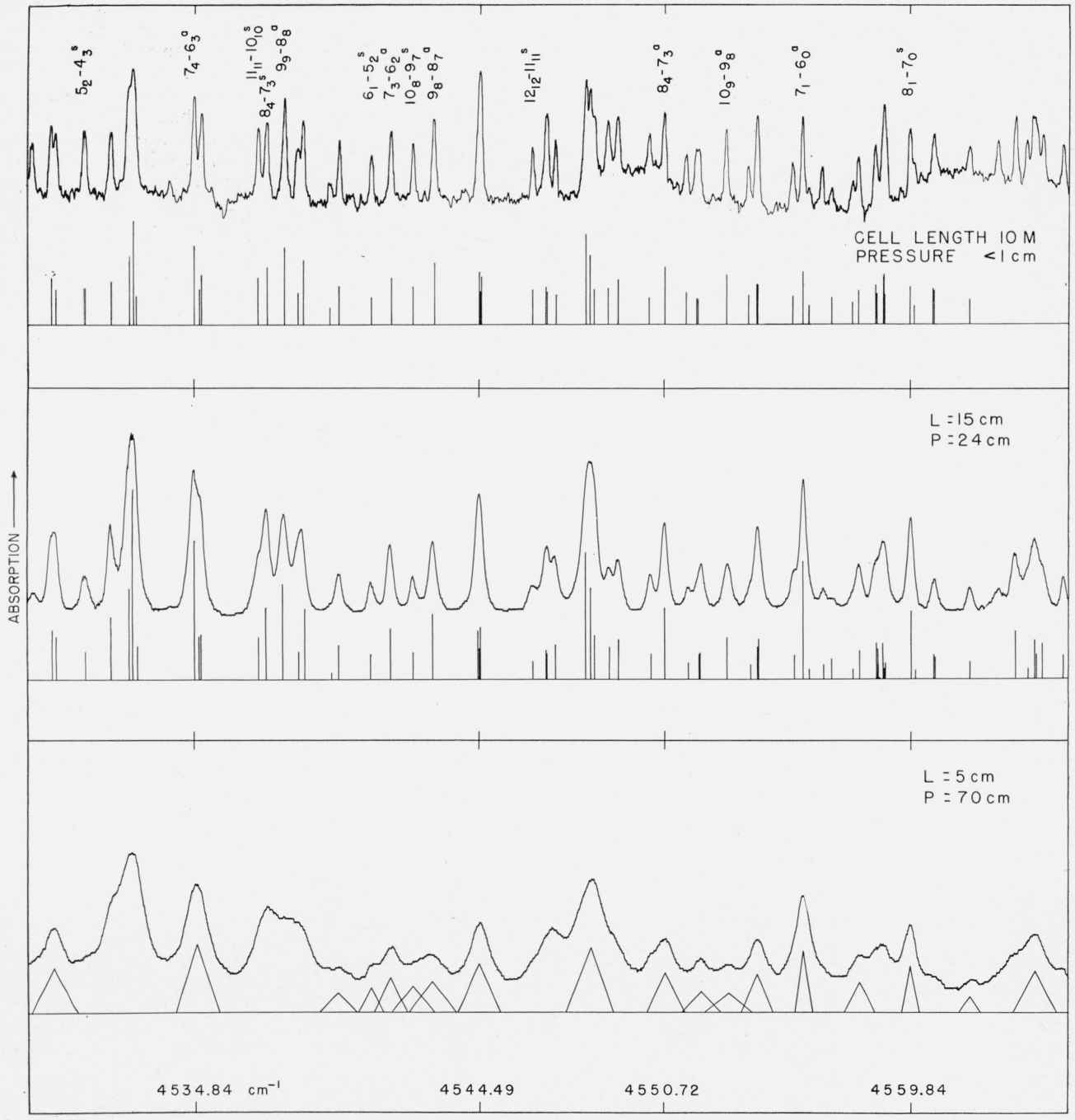

FIGURE 5. NH_3 *spectra, 4,530 to 4,560 cm^{-1}, at three path lengths.*

Upper spectrum, $p\sim$0.5 cm Hg; intensity $\sim(S\gamma)^{1/2}$; center spectrum, p=24 cm Hg, intensity $\sim S$; lower spectrum, p=70 cm Hg, width of intensity triangles $\sim\gamma$, height $\sim S/\gamma$.

broad lines, and thus to sort out lines with $K \sim 0$ from those with $K \sim J$ in otherwise unidentifiable situations. This technique proved of value in extending the analysis of the present bands to their highest J-values, where the series regularities became uncertain, and should also be very useful in beginning the analysis in very complicated bands, such as the higher overtone bands in the visible region [8] where there are many overlapping vibrational transitions with mutual perturbing interactions.

It may be noted that except for the effects of the considerable overlapping of lines in the "high-pressure" (70 cm Hg) tracings, the individual lines appear completely symmetrical about their central frequencies. Moreover, the central frequency does not shift detectably (<0.02 cm^{-1}) in the 70-cm pressure runs from its low-pressure value. This behavior confirms the lower-resolution finding of Nethercot and Peters [12], and has also been verified in all the NH_3 bands studied. It therefore would seem that the apparent shift and asymmetry of the microwave lines at pressures above 20 cm Hg [9] is a result of some property of the line shape when ν_0 and γ are of the same magnitude, rather than of any property of the statistical broadening of the energy levels.

Using the smoothed half-widths (table 10) and line strengths calculated from $S_v^0 = 19.7$ for $\nu_2+\nu_3$ and 2.9 for $\nu_1\nu_2$, a table of all the lines to be expected with the 1,000-cm path have been completed. A portion of the complete list is given as table 11, and, as pointed out earlier, the values of W_{calc} are proportional to the heights of the lines in figures 1 to 3. It is seen that a quite complete and accurate description of the spectrum has been attained. Only in the lower-frequency regions are there any considerable number of unassigned features, presumably due to other vibrational transitions such as $2\nu_4^0+\nu_2$, and $2\nu_4^2+\nu_2$. In the analyzed bands $\nu_1+\nu_2$ and $\nu_2+\nu_3$ both the positions and intensities are well accounted for.

TABLE 11. *Observed and calculated lines, 4,500 to 4,550 cm^{-1}*

ν		Line	100 S^0	γ^0	$(\epsilon_{max})i$ (1=5 cm)	W_L^0 (1=1,000 cm)	
Obs.	Calc.					Calc.	Obs.
cm^{-1}	cm^{-1}		cm^{-2} atm^{-1}	cm^{-1} atm^{-1}		cm^{-1} atm^{-1}	cm^{-1} atm^{-1}
4500.28	0.43	$^{Q}R(9,7)^{s}$	0.17	0.46	0.006	1.3	3.0
00.91	-----	----------	----------	----------	-----	----------	3.0
01.59	1.56	$^{R}R(4,3)^{a}$	20.7	.47	.70	18.3	21.4
	1.88	$^{Q}R(9,8)^{s}$	0.16	.50	.005	1.3	------
02.65	2.62	$^{R}R(5,3)^{s}$	12.9	.42	.49	14.7	12.0
03.11	3.11	$^{P}R(2,2)^{a}$	0.76	.38	.032	3.3	4.4
	3.30	$^{P}Q(11,11)^{a}$	.12	.53	.003	1.0	------
4503.72	3.67	$^{Q}R(9,9)^{s}$	.22	.53	.007	1.5	1.5
04.06	------	----------	----------	----------	------	------	2.5
04.44	------	----------	----------	----------	------	------	0.8
04.68	-----	----------	----------	----------	-----	-----	.3
04.94	4.96	$^{P}R(3,2)^{s}$	1.31	.32	.065	4.0	5.5
4505.56	5.50	$^{R}R(6,5)^{s}$	7.2	.51	.224	12.1	12.8
06.12	6.11	$^{R}R(5,5)^{a}$	13.2	.56	.374	15.2	15.2
08.16	8.20	$^{R}R(7,7)^{s}$	7.8	.57	.219	12.3	15.6
	8.23	$^{R}R(4,2)^{a}$	7.2	.38	.302	10.4	
09.10	-----	----------	----------	----------	-----	-----	0.3
09.42	9.25	$^{P}Q(12,12)^{a}$	0.09	.52	.003	0.8	.5
4510.05	0.06	$^{R}R(5,2)^{s}$	4.8	.35	.218	8.1	8.1
12.12	2.12	$^{R}R(5,4)^{a}$	9.2	.50	.290	13.5	11.9
	2.83	$^{R}R(6,4)^{s}$	5.1	.46	.178	9.5	
12.91	2.91	$^{P}R(3,1)^{a}$	2.53	.25	.161	5.0	18.8
	3.03	$^{P}R(3,3)^{s}$	0.94	.44	.033	3.9	
13.81	-----	----------	----------	----------	-----	-----	1.2
13.95	4.43?	$^{Q}R(10,6)^{s}$	.17	.40	.007	1.2	1.2
4515.19	5.18	$^{P}R(4,1)^{s}$	2.24	.24	.148	4.6	12.5
	5.22	$^{R}R(4,1)^{a}$	4.9	.29	.271	7.6	
15.55	5.58	$^{R}R(7,6)^{s}$	10.6	.51	.324	14.7	13.8
16.76	6.85	$^{R}R(6,6)^{a}$	21.0	.57	.589	21.9	21.0
17.34	7.57	$^{R}R(5,1)^{s}$	3.27	.28	.186	6.0	8.8
18.08	8.03	$^{R}R(8,8)^{s}$	5.3	.56	.150	10.8	13.8
4518.49	8.45	$^{R}R(5,3)^{a}$	12.7	.42	.48	14.6	14.4
19.37	8.69?	$^{Q}R(10,9)^{s}$	0.18	.49	.006	1.5	1.1
19.57	-----	----------	----------	----------	-----	-----	1.1
20.20	0.16	$^{R}R(6,3)^{s}$	7.2	.40	.289	10.7	8.8
21.01	0.97	$^{P}R(3,2)^{a}$	1.32	.32	.065	4.0	4.9
4522.43	2.42	$^{R}R(4,0)^{a}$	13.5	.24	.89	11.4	14.7
22.57	2.53	$^{R}R(6,5)^{a}$	7.2	.51	.225	12.1	13.5
22.87	2.84	$^{R}R(7,5)^{s}$	3.69	.46	.127	8.2	7.8
23.08	3.11	$^{P}R(4,2)^{s}$	1.40	.29	.077	4.0	5.1
23.97	-----	----------	----------	----------	-----	-----	0.4
4525.00	4.97	$^{R}R(5,0)^{s}$	9.7	.23	.674	9.4	13.5
	5.10	$^{R}R(5,2)^{a}$	4.8	.35	.219	8.1	
25.45	5.42	$^{R}R(8,7)^{s}$	3.53	.52	.108	8.5	7.3
25.87	6.14?	$^{Q}R(11,0)^{s}$	0.05	.17	.005	0.4	0.6
27.44	7.45	$^{R}R(7,7)^{a}$	7.8	.57	.218	13.2	
	7.52	$^{R}R(6,2)^{s}$	2.72	.34	.127	6.0	28.9
27.59	7.56	$^{R}R(9,9)^{s}$	7.1	.55	.205	12.4	

TABLE 11. *Observed and calculated lines, 4,500 to 4,550 cm^{-1}*—Continued

ν		Line	100 S^0	γ^0	$(\epsilon_{max})i$ (1=5 cm)	$W_L{}^0$ (1=1,000 cm)	
Obs.	Calc.					Calc.	Obs.
cm^{-1}	cm^{-1}		cm^{-2} atm^{-1}	cm^{-1} atm^{-1}		$cm^{-1}atm^{-1}$	$cm^{-1}atm^{-1}$
4528.55	8.53	$^RR(6,4)^a$	5.2	.46	.179	9.5	7.6
29.45	9.46	$^PR(3,3)^a$	0.94	.44	.033	3.9	4.0
30.01	0.05	$^RR(7,4)^s$	2.63	.41	.096	6.5	6.8
30.21	.24	$^PR(4,1)^a$	2.24	.24	.148	4.6	6.2
31.17	1.16	$^PR(4,3)^s$	1.49	.38	.062	4.7	5.6
4532.06	2.07	$^RR(5,1)^a$	3.28	.28	.186	6.0	6.2
32.66	2.63	$^RR(8,6)^s$	4.8	.47	.161	9.5	}
32.79	{ 2.79	$^RR(7,6)^a$	10.6	.51	.325	14.7	} 30.4
	{ 2.93	$^PR(5,1)^s$	2.15	.23	.153	4.4	}
34.03	3.46?	$^QR(11,9)^s$	0.08	.46	.003	0.7	1.1
34.84	4.83	$^RR(6,3)^a$	7.3	.40	.290	10.7	9.6
4535.07	{ 4.96	$^RR(6,1)^s$	2.06	.27	.121	4.7	} 8.1
	{ 5.04	$^RR(9,8)^s$	2.16	.52	.066	6.6	}
35.53	5.30?	$^QR(11,10)^s$	0.04	.49	.001	0.4	0.9
36.95	6.92	$^RR(10,10)^s$	1.97	.55	.050	6.4	6.2
37.23	7.24	$^RR(7,3)^s$	3.76	.37	.161	7.4	7.1
37.86	7.89	$^RR(8,8)^a$	5.3	.56	.151	10.8	10.1
4538.32	8.28	$^PR(4,2)^a$	1.40	.29	.077	4.0	6.7
38.48	8.46	$^RR(7,5)^a$	3.70	.46	.127	8.2	7.8
39.05	-----	-----	-----	-----	-----	-----	0.8
39.39	9.38	$^PR(4,4)^s$	0.28	.47	.009	1.9	1.7
39.73	9.73	$^RR(8,5)^s$	1.75	.42	.066	5.3	5.4
4540.18	-----	-----	-----	-----	-----	-----	1.1
40.82	0.84	$^PR(5,2)^s$	1.16	.28	.066	3.5	4.0
41.46	1.46	$^RR(6,2)^a$	2.73	.34	.127	6.0	6.8
42.23	2.21	$^RR(9,7)^s$	1.44	.48	.048	5.1	5.4
42.90	2.90	$^RR(8,7)^a$	3.54	.52	.108	8.5	7.2
4543.94	-----	-----	-----	-----	-----	-----	0.9
	{ 4.42	$^RR(10,9)^s$	2.52	.51	.079	7.1	}
44.49	{ 4.44	$^RR(7,2)^s$	1.45	.31	.075	2.1	} 18.5
	{ 4.54	$^RR(7,4)^a$	2.64	.41	.096	6.5	}
46.31	5.95	$^RR(11,11)^s$	1.08	.54	.032	4.7	4.1
46.76	{ 6.73	$^PR(4,3)^a$	1.49	.38	.064	4.7	} 10.7
	{ 6.80	$^RR(8,4)^s$	1.25	.38	.053	4.3	}
47.06	7.05	$^PR(5,1)^a$	2.15	.23	.153	4.4	5.0
4548.12	8.05	$^RR(9,9)^a$	7.1	.55	.206	12.4	7.9
48.29	8.26	$^RR(8,6)^a$	4.8	.47	.162	9.5	6.2
48.41	8.41	$^RR(6,1)^a$	2.07	.27	.121	4.7	3.4
48.83	8.90	$^PR(5,3)^s$	1.50	.35	.068	4.5	5.6
49.18	9.23	$^RR(9,6)^s$	2.04	.44	.074	5.9	6.0

4. Summary and Conclusions

A quite complete analysis has been obtained of the two strongest combination bands of NH_3 in the region of 2.3 microns. Accurate rotational constants for the ground state have been derived, and for the upper state good values have been obtained for the basic rotational constants, and in addition fine details of the energy levels involving the interaction of the inversion splitting and rotation, and of the Coriolis interaction constants and rotation have been noted. The intensities and collision half-widths of the lines, and the variation of these parameters with rotational state, have also been obtained.

Similar studies have been made of a number of other bands of NH_3 and its isotopic modifications at wavelengths shorter than 6 microns. These results, and derivation therefrom of basic structural paramters of the ammonia molecule, will be reported in subsequent papers.

5. References

[1] D. M. Dennison, Revs. Modern Phys. **12,** 175 (1940).
[2] H. Y. Sheng, E. F. Barker, and D. M. Dennison, Phys. Rev. **60,** 786 (1941).
[3] C. Cumming, Can. J. Phys. **33,** 635 (1955).
[4] E. F. Barker, Phys. Rev. **55,** 657 (1939).
[5] S. C. Chao, Phys. Rev. **50,** 27 (1936).
[6] C. F. Townes and A. W. Schawlow, Microwave spectroscopy (McGraw-Hill Publishing Co., Inc., New York, N. Y., 1956).
[7] W. S. Benedict, R. C. Herman, G. E. Moore, and S. Silverman, Can. J. Phys. **34,** 830 (1956).
[8] P. W. Anderson, Phys. Rev. **76,** 647 (1949).
[9] B. Bleaney and R. P. Penrose, Proc. Phys. Soc. (London) **60,** 548 (1948).
[10] J. H. Van Vleck and V. M. Weisskopf, Rev. Modern Phys. **17,** 227 (1948).
[11] H. Margenau, Phys. Rev. **76,** 1423 (1949).
[12] A. H. Nethercot, Jr., and C. W. Peters, Phys. Rev. **79,** 225 (1950).
[13] W. S. Benedict and E. K. Plyler, J. Chem. Phys. **24,** 904 (1956); Symposium on molecular structure and spectroscopy (The Ohio State University, Columbus, Ohio, 1956, 1957).
[14] H. H. Nielsen, Revs. Modern Phys. **23,** 90 (1951).
[15] R. S. Mulliken, J. Chem. Phys. **23,** 1997 (1955).
[16] H. H. Nielsen and D. M. Dennison, Phys. Rev. **72,** 1101 (1947).
[17] C. C. Costain, Phys. Rev. **82,** 108 (1951).
[18] G. Herzberg, Infrared and raman spectra (D. Van Nostrand Co., New York, N. Y., 1945).
[19] H. Hansen and H. H. Nielsen, Symposium on molecular structure and spectroscopy (The Ohio State University, Columbus, Ohio, 1957).
[20] D. C. McKean and P. N. Schatz, J. Chem. Phys. **24,** 316 (1956).
[21] H. J. Kostkowski and A. M. Bass, J. Opt. Soc. Am. **46,** 1060 (1956).

WASHINGTON, December 3, 1957.